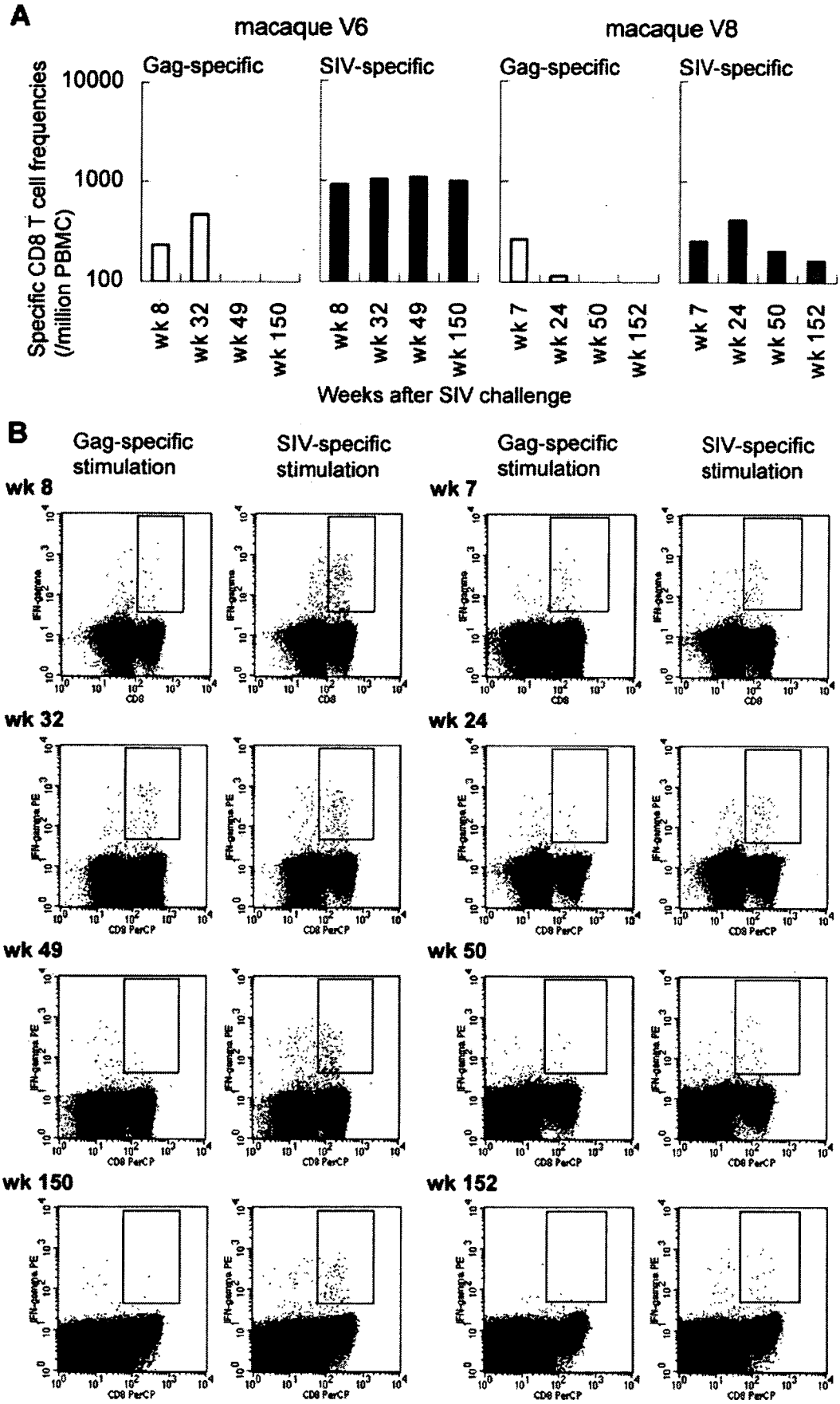

FIG. 3. Virus-specific $CD8^+$ T-cell responses in sustained controllers V6 (left panels) and V8 (right panels). (A) Gag-specific and SIV-specific $CD8^+$ T-cell frequencies in PBMCs. (B) Dot plots gated on $CD3^+$ lymphocytes after Gag-specific or SIV-specific stimulation.

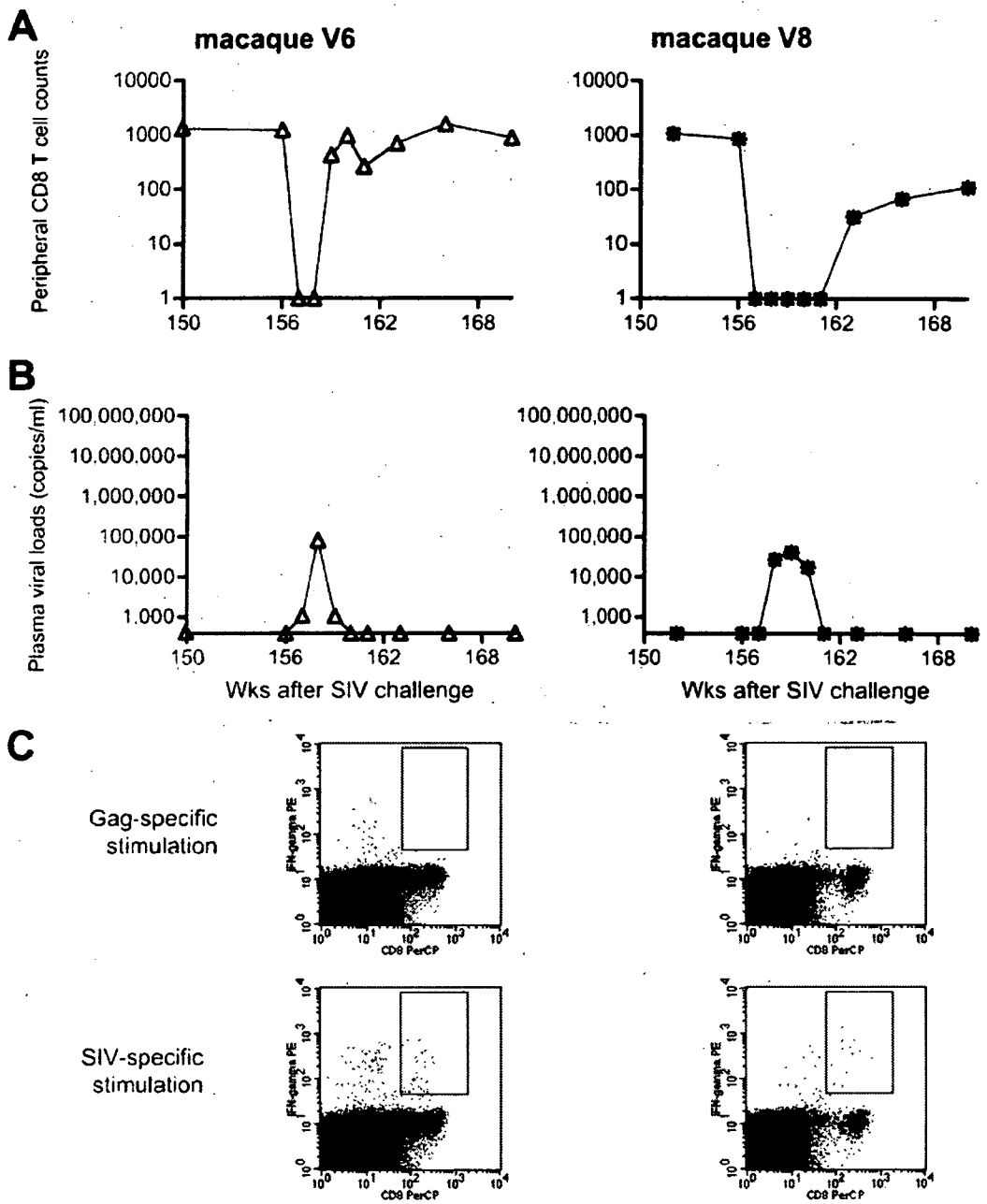

FIG. 4. $CD8^+$ cell depletion experiments starting at week 156 in sustained controllers V6 (left panels) and V8 (right panels). (A) Peripheral $CD8^+$ T-cell counts (per μl). (B) Plasma viral loads (viral RNA copies/ml plasma). (C) Virus-specific CTL responses at week 160 in V6 and at week 166 in V8. Dot plots gated on $CD3^+$ lymphocytes after Gag-specific or SIV-specific stimulation are shown.

to week 70. At approximately week 120, all the sustained controllers still showed preservation of memory and central memory $CD4^+$ T cells. In contrast, both of the transient controllers, V3 and V5, experienced a reduction in central memory $CD4^+$ T-cell counts, although reduction in memory $CD4^+$ T-cell counts was observed in only one of them. These results suggest that CTL-based vaccines that control viral replication can also preserve central memory $CD4^+$ T cells even in the chronic phase. Finally, statistical analysis revealed that there was no significant reduction in central memory $CD4^+$ T cells during the period between weeks 12 and 70 in the controllers (Fig. 6). Thus, CTL vaccine-based, sustained viral control can result in preservation of central memory $CD4^+$ T cells in both the chronic phase as well as the acute phase.

DISCUSSION

Here we followed three Burmese rhesus macaques that maintained CTL vaccine-based control of SIVmac239 replication without disease progression for more than 3 years. The

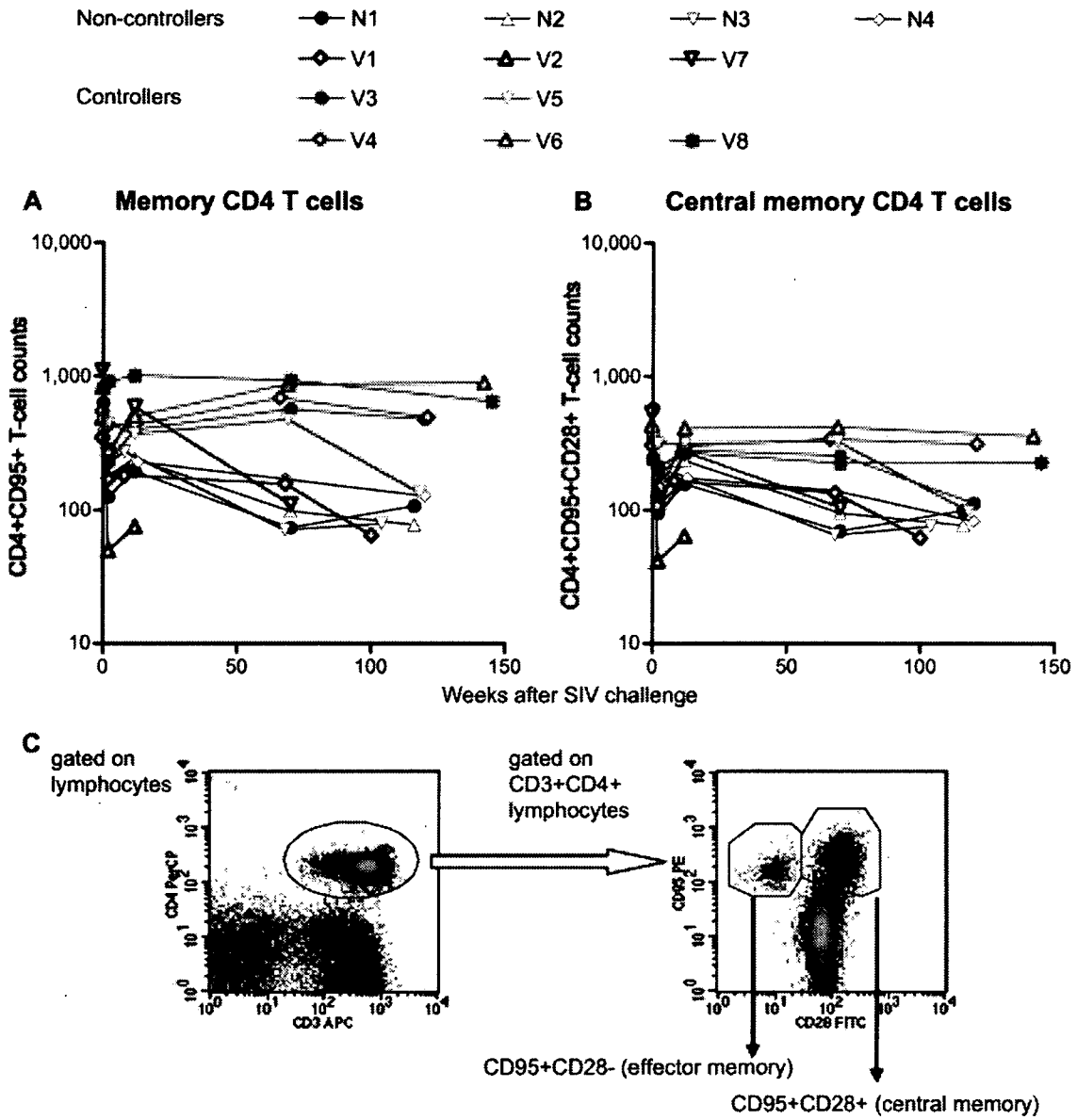

FIG. 5. Changes in peripheral memory $CD4^+$ T-cell counts. Noncontrollers are indicated in black or blue, and controllers are indicated in red. (A) Peripheral memory $CD4^+$ ($CD4^+$ $CD95^-$) T-cell counts (per μl). (B) Peripheral central memory $CD4^+$ ($CD4^-$ $CD95^+$ $CD28^+$) T-cell counts (per μl). (C) Representative density plots (macaque V4 prechallenge) for determining peripheral memory $CD4^+$ T-cell percentages. The left panel is a density plot gated on lymphocytes, and in this plot, $CD3^+$ $CD4^+$ lymphocytes are gated for the right panel of the density plot. In the right panel, we determined the percentages of central memory ($CD95^+$ $CD28^+$) $CD4^+$ T cells and memory ($CD95^-$ $CD28^+$ plus $CD95^-$ $CD28^-$) $CD4^+$ T cells.

set-point plasma viral loads in SIVmac239-infected Burmese rhesus macaques may be lower than those usually observed in SIVmac239-infected Indian rhesus but are higher than those typically observed in untreated humans infected with HIV-1. All four of the naive control animals along with three vaccinees failed to control viremia after SIVmac239 challenge. They also experienced peripheral $CD4^+$ T-cell loss and developed AIDS in 3 years, indicating that this model of SIVmac239 infection in Burmese rhesus macaques is adequate for evaluation of vaccine efficacies. Our finding of long-term control of viral replication and $CD4^+$ T-cell preservation in three vaccinees in this AIDS model underlines the potential of a prophylactic CTL-based vaccine for AIDS prevention.

Our previous study revealed rapid selection of Gag CTL escape mutations in all the controllers, indicating that vaccine-induced Gag-specific CTL responses played an important role in viral control in the early phase of SIV infection (17). In the chronic phase, neutralizing antibody induction was still inefficient, and our results suggest long-term CTL-based viral containment. Indeed, the vaccine-induced Gag-specific CTL responses have been shown to play a crucial role in viral control even in the chronic phase in one (V4) of three sustained

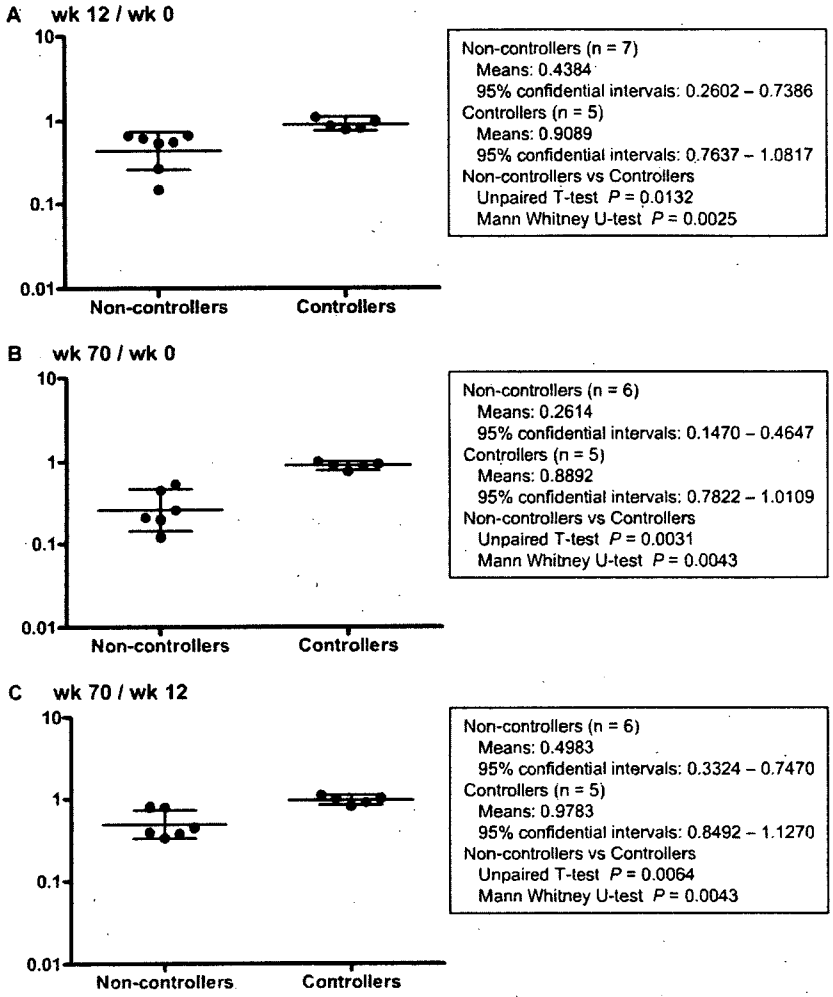

FIG. 6. Statistical analysis indicating preservation of central memory $CD4^+$ T-cell counts in the controllers. The ratios of central memory $CD4^+$ T-cell counts at week 12 to week 0 (A), week 70 to week 0 (B), and week 70 to week 12 (C) in the noncontrollers (except for rapid progressor V2 in panels B and C) and the controllers are plotted. The longer bars indicate geometric mean values, and the regions between the shorter bars indicate the 95% confidential intervals. Statistical analysis was performed with the *t* test and nonparametric Mann-Whitney U-test using the Prizm software.

controllers (10). In contrast, Gag-specific CTL responses became undetectable and SIV non-Gag-specific CTL responses, instead, became predominant in macaques V6 and V8. The results obtained from a $CD8^+$ cell depletion experiment are consistent with involvement of these SIV non-Gag-specific CTL responses in the long-term viral control in both sustained controllers, although there might be involvement of other components, such as NK and $CD4^+$ memory T cells. Thus, it can be speculated that vaccine-based control of primary SIV replication can preserve the ability of the immune system to elicit functional CTL responses, leading to reinforcement or adaptation of protective immunity by postchallenge induction or expansion of effective CTL responses. This may contribute to stable viral containment in the chronic phase.

In the natural courses of HIV and SIV infections, the infected hosts exhibit acute, massive depletion of $CCR5^+$ $CD4^+$ effector memory T cells from mucosal effector sites, and the chronic immune activation with gradual immune disruption that follows leads to AIDS (7, 15, 20, 25). The former acute memory loss may influence the latter chronic disease progression (25, 26). The acute depletion results in compromised immune responses at the effector sites and systemic proliferative responses that partially compensate for the loss of mucosal memory $CD4^+$ T-cell populations. Recent reports indicating amelioration of acute mucosal memory $CD4^+$ T-cell depletion and associated central memory $CD4^+$ T-cell loss in the early phase by CTL-based vaccines have suggested that vaccine-based amelioration of acute memory $CD4^+$ T-cell depletion in mucosal effector sites can delay AIDS progression (13, 19, 35). However, this acute memory $CD4^+$ T-cell depletion is not the only cause of chronic disease progression and persistent viral replication-associated immune activation may be responsible for chronic immune disruption leading to AIDS (7). Indeed, in both of the transient controllers, V3 and V5, central memory $CD4^+$ T cells were preserved during the initial, transient period of viremia control but decreased after the reappearance of plasma viremia. This suggests that there may be an association between persistent viral con-

tainment and central memory $CD4^+$ T-cell preservation, even in the chronic phase.

Theoretically, protection by CTL-based AIDS vaccines is likely to be nonsterile, and it will be difficult to contain viral replication completely. Additionally, CTL-based viremia control would require CTL activation. Indeed, our $CD8^+$ cell depletion experiment indicated that persistent viral replication was inefficient but not completely contained in the absence of plasma viremia in sustained controllers V6 and V8. Transition of recognition of CTL epitopes from Gag to other non-Gag proteins in the chronic phase suggests that these "new" CTLs were either elicited or expanded by viral replication in the acute phase or by this inefficient persistent viral replication. Nevertheless, these macaques showed long-term viral control with central memory $CD4^+$ T-cell preservation, indicating that nonsterile protection by CTL-based vaccines can result in prevention of chronic central memory $CD4^+$ T-cell loss.

In summary, the present study shows that primary viral control by a CTL-based AIDS vaccine can result in long-term control of SIV replication by adapted CTL responses and preservation of central memory $CD4^+$ T cells without AIDS progression. Our results suggest that CTL-based vaccines can result in long-term viral containment and disease control.

ACKNOWLEDGMENTS

This work was supported by a grant from the Ministry of Education, Culture, Sports, Science, and Technology, grants from the Japan Health Sciences Foundation, and grants from the Ministry of Health, Labor, and Welfare in Japan.

The animal experiments were conducted through the Cooperative Research Program in Tsukuba Primate Research Center, National Institute of Biomedical Innovation with the help of the Corporation for Production and Research of Laboratory Primates. We thank Centocor Inc. and K. A. Reimann for providing cM-T807 and DNAVEC Corp. and J. Lifson, Y. Ami, F. Ono, K. Komatsuzaki, A. Hiyaoka, A. Oyama, K. Oto, H. Oto, H. Akari, K. Terao, M. Miyazawa, M. Yasunami, A. Kimura, M. Takiguchi, A. Kato, K. Mori, N. Yamamoto, T. Takemori, T. Sata, T. Kurata, K. Koike, Y. Nagai, and A. Nomoto for their help.

REFERENCES

1. **Amara, R. R., F. Villinger, J. D. Altman, S. L. Lydy, S. P. O'Neil, S. I. Staprans, D. C. Montefiori, Y. Xu, J. G. Herndon, L. S. Wyatt, M. A. Caudido, N. L. Kozyr, P. L. Earl, J. M. Smith, H. L. Ma, B. D. Grimm, M. L. Hulsey, J. Miller, H. M. McClure, J. M. McNicholl, B. Moss, and H. L. Robinson.** 2001. Control of a mucosal challenge and prevention of AIDS in rhesus macaques by a multiprotein DNA/MVA vaccine. Science **292**:69–74.
2. **Arguello, J. R., A. M. Little, A. L. Pay, D. Gallardo, I. Rojas, S. G. Marsh, J. M. Goldman, and J. A. Madrigal.** 1998. Mutation detection and typing of polymorphic loci through double-strand conformation analysis. Nat. Genet. **18**:192–194.
3. **Borrow, P., H. Lewicki, B. H. Hahn, G. M. Shaw, and M. B. Oldstone.** 1994. Virus-specific $CD8^+$ cytotoxic T-lymphocyte activity associated with control of viremia in primary human immunodeficiency virus type 1 infection. J. Virol. **68**:6103–6110.
4. **Casimiro, D. R., F. Wang, W. A. Schleif, X. Liang, Z. Q. Zhang, T. W. Tobery, M. E. Davies, A. B. McDermott, D. H. O'Connor, A. Fridman, A. Bagchi, L. G. Tussey, A. J. Bett, A. C. Finnefrock, T. M. Fu, A. Tang, K. A. Wilson, M. Che, H. C. Perry, G. J. Heidecker, D. C. Freed, A. Carella, K. S. Punt, K. J. Sykes, L. Huang, V. I. Ausensi, M. Bachinsky, U. Sadasivan-Nair, D. I. Watkins, E. A. Emini, and J. W. Shiver.** 2005. Attenuation of simian immunodeficiency virus SIVmac239 infection by prophylactic immunization with DNA and recombinant adenoviral vaccine vectors expressing Gag. J. Virol. **79**:15547–15555.
5. **Feinberg, M. B., and J. P. Moore.** 2002. AIDS vaccine models: challenging challenge viruses. Nat. Med. **8**:207–210.
6. **Goulder, P. J., and D. I. Watkins.** 2004. HIV and SIV CTL escape: implications for vaccine design. Nat. Rev. Immunol. **4**:630–640.
7. **Grossman, Z., M. Meier-Schellersheim, W. E. Paul, and L. J. Picker.** 2006. Pathogenesis of HIV infection: what the virus spares is as important as what it destroys. Nat. Med. **12**:289–295.
8. **Jin, X., D. E. Bauer, S. E. Tuttleton, S. Lewin, A. Gettie, J. Blanchard, C. E. Irwin, J. T. Safrit, J. Mittler, L. Weinberger, L. G. Kostrikis, L. Zhang, A. S. Perelson, and D. D. Ho.** 1999. Dramatic rise in plasma viremia after $CD8^+$ T cell depletion in simian immunodeficiency virus-infected macaques. J. Exp. Med. **189**:991–998.
9. **Kato, A., Y. Sakai, T. Shioda, T. Kondo, M. Nakanishi, and Y. Nagai.** 1996. Initiation of Sendai virus multiplication from transfected cDNA or RNA with negative or positive sense. Genes Cells **1**:569–579.
10. **Kawada, M., H. Igarashi, A. Takeda, T. Tsukamoto, H. Yamamoto, S. Dohki, M. Takiguchi, and T. Matano.** 2006. Involvement of multiple epitope-specific cytotoxic T-lymphocyte responses in vaccine-based control of simian immunodeficiency virus replication in rhesus macaques. J. Virol. **80**:1949–1958.
11. **Kestler, H. W., III, D. J. Ringler, K. Mori, D. L. Panicali, P. K. Sehgal, M. D. Daniel, and R. C. Desrosiers.** 1991. Importance of the nef gene for maintenance of high virus loads and for development of AIDS. Cell **65**:651–662.
12. **Koup, R. A., J. T. Safrit, Y. Cao, C. A. Andrews, G. McLeod, W. Borkowsky, C. Farthing, and D. D. Ho.** 1994. Temporal association of cellular immune responses with the initial control of viremia in primary human immunodeficiency virus type 1 syndrome. J. Virol. **68**:4650–4655.
13. **Letvin, N. L., J. R. Mascola, Y. Sun, D. A. Gorgone, A. P. Buzby, L. Xu, Z. Y. Yang, B. Chakrabarti, S. S. Rao, J. E. Schmitz, D. C. Montefiori, B. R. Barker, F. L. Bookstein, and G. J. Nabel.** 2006. Preserved $CD4^+$ central memory T cells and survival in vaccinated SIV-challenged monkeys. Science **312**:1530–1533.
14. **Li, H. O., Y. F. Zhu, M. Asakawa, H. Kuma, T. Hirata, Y. Ueda, Y. S. Lee, M. Fukumura, A. Iida, A. Kato, Y. Nagai, and M. Hasegawa.** 2000. A cytoplasmic RNA vector derived from nontransmissible Sendai virus with efficient gene transfer and expression. J. Virol. **74**:6564–6569.
15. **Li, Q., L. Duan, J. D. Estes, Z. M. Ma, T. Rourke, Y. Wang, C. Reilly, J. Carlis, C. J. Miller, and A. T. Haase.** 2005. Peak SIV replication in resting memory $CD4^+$ T cells depletes gut lamina propria $CD4^+$ T cells. Nature **434**:1148–1152.
16. **Matano, T., M. Kano, H. Nakamura, A. Takeda, and Y. Nagai.** 2001. Rapid appearance of secondary immune responses and protection from acute CD4 depletion after a highly pathogenic immunodeficiency virus challenge in macaques vaccinated with a DNA-prime/Sendai viral vector-boost regimen. J. Virol. **75**:11891–11896.
17. **Matano, T., M. Kobayashi, H. Igarashi, A. Takeda, H. Nakamura, M. Kano, C. Suginoto, K. Mori, A. Iida, T. Hirata, M. Hasegawa, T. Yuasa, M. Miyazawa, Y. Takahashi, M. Yasunami, A. Kimura, D. H. O'Connor, D. I. Watkins, and Y. Nagai.** 2004. Cytotoxic T lymphocyte-based control of simian immunodeficiency virus replication in a preclinical AIDS vaccine trial. J. Exp. Med. **199**:1709–1718.
18. **Matano, T., R. Shibata, C. Siemon, M. Connors, H. C. Lane, and M. A. Martin.** 1998. Administration of an anti-CD8 monoclonal antibody interferes with the clearance of chimeric simian/human immunodeficiency virus during primary infections of rhesus macaques. J. Virol. **72**:164–169.
19. **Mattapallil, J. J., D. C. Douek, A. Buckler-White, D. C. Montefiori, N. L. Letvin, G. J. Nabel, and M. Roederer.** 2006. Vaccination preserves CD4 memory T cells during acute simian immunodeficiency virus challenge. J. Exp. Med. **203**:1533–1541.
20. **Mattapallil, J. J., D. C. Douek, B. Hill, Y. Nishimura, M. A. Martin, and M. Roederer.** 2005. Massive infection and loss of memory $CD4^+$ T cells in multiple tissues during acute SIV infection. Nature **434**:1093–1097.
21. **McMichael, A. J., and T. Hanke.** 2003. HIV vaccines 1983–2003. Nat. Med. **9**:874–880.
22. **Nishimura, Y., C. R. Brown, J. J. Mattapallil, T. Igarashi, A. Buckler-White, B. A. Lafont, V. M. Hirsch, M. Roederer, and M. A. Martin.** 2005. Resting naive $CD4^+$ T cells are massively infected and eliminated by X4-tropic simian-human immunodeficiency viruses in macaques. Proc. Natl. Acad. Sci. USA **102**:8000–8005.
23. **Nishimura, Y., T. Igarashi, O. K. Donau, A. Buckler-White, C. Buckler, B. A. Lafont, R. M. Goeken, S. Goldstein, V. M. Hirsch, and M. A. Martin.** 2004. Highly pathogenic SHIVs and SIVs target different $CD4^+$ T cell subsets in rhesus monkeys, explaining their divergent clinical courses. Proc. Natl. Acad. Sci. USA **101**:12324–12329.
24. **Ogg, G. S., X. Jin, S. Bonhoeffer, P. R. Dunbar, M. A. Nowak, S. Monard, J. P. Segal, Y. Cao, S. L. Rowland-Jones, V. Cerundolo, A. Hurley, M. Markowitz, D. D. Ho, D. F. Nixon, and A. J. McMichael.** 1998. Quantitation of HIV-1-specific cytotoxic T lymphocytes and plasma load of viral RNA. Science **279**:2103–2106.
25. **Picker, L. J., and D. I. Watkins.** 2005. HIV pathogenesis: the first cut is the deepest. Nat. Immunol. **6**:430–432.
26. **Picker, L. J., S. I. Hagen, R. Lum, E. F. Reed-Inderbitzin, L. M. Daly, A. W. Sylwester, J. M. Walker, D. C. Siess, M. Piatak, Jr., C. Wang, D. B. Allison, V. C. Maino, J. D. Lifson, T. Kodama, and M. K. Axthelm.** 2004. Insufficient production and tissue delivery of $CD4^+$ memory T cells in rapidly progressive simian immunodeficiency virus infection. J. Exp. Med. **200**:1299–1314.
27. **Pitcher, C. J., S. I. Hagen, J. M. Walker, R. Lum, B. L. Mitchell, V. C. Maino, M. K. Axthelm, and L. J. Picker.** 2004. Development and homeostasis of T cell memory in rhesus macaques. J. Immunol. **168**:29–43.

28. **Rose, N. F., P. A. Marx, A. Luckay, D. F. Nixon, W. J. Moretto, S. M. Donahoe, D. Montefiori, A. Roberts, L. Buonocore, and J. K. Rose.** 2001. An effective AIDS vaccine based on live attenuated vesicular stomatitis virus recombinants. Cell **106**:539–549.
29. **Schmitz, J. E., M. J. Kuroda, S. Santra, V. G. Sasseville, M. A. Simon, M. A. Lifton, P. Racz, K. Tenner-Racz, M. Dalesandro, B. J. Scallon, J. Ghrayeb, M. A. Forman, D. C. Montefiori, E. P. Rieber, N. L. Letvin, and K. A. Reimann.** 1999. Control of viremia in simian immunodeficiency virus infection by $CD8^+$ lymphocytes. Science **283**:857–860.
30. **Shibata, R., F. Maldarelli, C. Siemon, T. Matano, M. Parta, G. Miller, T. Fredrickson, and M. A. Martin.** 1997. Infection and pathogenicity of chimeric simian-human immunodeficiency viruses in macaques: determinants of high virus loads and CD4 cell killing. J. Infect. Dis. **176**:362–373.
31. **Shiver, J. W., T. M. Fu, L. Chen, D. R. Casimiro, M. E. Davies, R. K. Evans, Z. Q. Zhang, A. J. Simon, W. L. Trigona, S. A. Dubey, L. Huang, V. A. Harris, R. S. Long, X. Liang, L. Handt, W. A. Schleif, L. Zhu, D. C. Freed, N. V. Persaud, L. Guan, K. S. Punt, A. Tang, M. Chen, K. A. Wilson, K. B. Collins, G. J. Heidecker, V. R. Fernandez, H. C. Perry, J. G. Joyce, K. M. Grimm, J. C. Cook, P. M. Keller, D. S. Kresock, H. Mach, R. D. Troutman, L. A. Isopi, D. M. Williams, Z. Xu, K. E. Bohannon, D. B. Volkin, D. C. Montefiori, A. Miura, G. R. Krivulka, M. A. Lifton, M. J. Kuroda, J. E. Schmitz, N. L. Letvin, M. J. Caulfield, A. J. Bett, R. Youil, D. C. Kaslow, and E. A. Emini.** 2002. Replication-incompetent adenoviral vaccine vector elicits effective anti-immunodeficiency-virus immunity. Nature **415**: 331–335.
32. **Takeda, A., H. Igarashi, H. Nakamura, M. Kano, A. Iida, T. Hirata, M. Hasegawa, Y. Nagai, and T. Matano.** 2003. Protective efficacy of an AIDS vaccine, a single DNA-prime followed by a single booster with a recombinant replication-defective Sendai virus vector, in a macaque AIDS model. J. Virol. **77**:9710–9715.
33. **Veazey, R. S., K. G. Mansfield, I. C. Tham, A. C. Carville, D. E. Shvetz, A. E. Forand, and A. A. Lackner.** 2000. Dynamics of CCR5 expression by $CD4^+$ T cells in lymphoid tissues during simian immunodeficiency virus infection. J. Virol. **74**:11001–11007.
34. **Veazey, R. S., M. DeMaria, L. V. Chalifoux, D. E. Shvetz, D. R. Pauley, H. L. Knight, M. Rosenzweig, R. P. Johnson, R. C. Desrosiers, and A. A. Lackner.** 1998. Gastrointestinal tract as a major site of $CD4^+$ T cell depletion and viral replication in SIV infection. Science **280**:427–431.
35. **Wilson, N. A., J. Reed, G. S. Napoe, S. Piaskowski, A. Szymanski, J. Furlott, E. J. Gonzalez, L. J. Yant, N. J. Maness, G. E. May, T. Soma, M. R. Reynolds, E. Rakasz, R. Rudersdorf, A. B. McDermott, D. H. O'connor, T. C. Friedrich, D. B. Allison, A. Patki, L. J. Picker, D. R. Burton, J. Lin, L. Huang, D. Patel, G. Heindecker, J. Fan, M. Citron, M. Horton, F. Wang, X. Liang, J. W. Shiver, D. R. Casimiro, and D. I. Watkins.** 2006. Vaccine-induced cellular immune responses reduce plasma viral concentrations after repeated low-dose challenge with pathogenic simian immunodeficiency virus SIVmac239. J. Virol. **80**:5875–5885.

Post-Infection Immunodeficiency Virus Control by Neutralizing Antibodies

Hiroyuki Yamamoto[1,2], Miki Kawada[1,2], Akiko Takeda[1], Hiroko Igarashi[2], Tetsuro Matano[1,2,3,4]*

1 International Research Center for Infectious Diseases, The Institute of Medical Science, The University of Tokyo, Tokyo, Japan, 2 Graduate School of Medicine, The University of Tokyo, Tokyo, Japan, 3 AIDS Research Center, National Institute of Infectious Diseases, Tokyo, Japan, 4 Tsukuba Primate Research Center, National Institute of Biomedical Innovation, Ibaraki, Japan

Background. **Unlike most acute viral infections controlled with the appearance of virus-specific neutralizing antibodies (NAbs), primary HIV infections are not met with such potent and early antibody responses. This brings into question if or how the presence of potent antibodies can contribute to primary HIV control, but protective efficacies of antiviral antibodies in primary HIV infections have remained elusive; and, it has been speculated that even NAb induction could have only a limited suppressive effect on primary HIV replication once infection is established. Here, in an attempt to answer this question, we examined the effect of passive NAb immunization post-infection on primary viral replication in a macaque AIDS model.** ***Methods and Findings.*** **The inoculums for passive immunization with simian immunodeficiency virus mac239 (SIVmac239)-specific neutralizing activity were prepared by purifying polyclonal immunoglobulin G from pooled plasma of six SIVmac239-infected rhesus macaques with NAb induction in the chronic phase. Passive immunization of rhesus macaques with the NAbs at day 7 after SIVmac239 challenge resulted in significant reduction of set-point plasma viral loads and preservation of central memory CD4 T lymphocyte counts, despite the limited detection period of the administered NAb responses. Peripheral lymph node dendritic cell (DC)-associated viral RNA loads showed a remarkable peak with the NAb administration, and DCs stimulated in vitro with NAb-preincubated SIV activated virus-specific CD4 T lymphocytes in an Fc-dependent manner, implying antibody-mediated virion uptake by DCs and enhanced T cell priming.** ***Conclusions.*** **Our results present evidence indicating that potent antibody induction post-infection can result in primary immunodeficiency virus control and suggest direct and indirect contribution of its absence to initial control failure in HIV infections. Although difficulty in achieving requisite neutralizing titers for sterile HIV protection by prophylactic vaccination has been suggested, this study points out a possibility of non-sterile HIV control by prophylactic vaccine-induced, sub-sterile titers of NAbs post-infection, providing a rationale of vaccine-based NAb induction for primary HIV control.**

Citation: Yamamoto H, Kawada M, Takeda A, Igarashi H, Matano T (2007) Post-Infection Immunodeficiency Virus Control by Neutralizing Antibodies. PLoS ONE 2(6): e540. doi:10.1371/journal.pone.0000540

INTRODUCTION

In the natural courses of HIV infections, the host immune responses fail to contain the virus replication and allow persistent plasma viremia. While virus-specific cytotoxic T lymphocyte (CTL) responses exert strong suppressive pressure on primary HIV replication [1–7], the contribution of virus-specific antibodies in clearance of primary HIV infection has remained unclear [8].

Neutralizing antibodies (NAbs) play a central role in control of most viral infections, but in HIV infections, NAb induction is not efficient in the early phase due to its unusual neutralization-resistant nature, such as the sophisticated masking of neutralizing epitopes in HIV envelope [8–11], and protective efficacies of post-infection NAbs in vivo have remained elusive. While evidence of virus escape implies NAb selective pressure to a certain extent [10,12–13], it has been speculated that post-infection NAbs could exert only a limited suppressive effect on primary HIV replication [14–16].

Post-infection passive NAb immunization studies in macaque AIDS models would contribute to elucidation of its protective role, in complementation with studies determining the requisites for sterile protection by pre-challenge administered NAb titers [14,16–21]. A model of CCR5-tropic simian immunodeficiency virus (SIV) infection that induces acute loss of memory $CD4^+$ T cells like HIV infections in humans [22–25] would be adequate for assessment of post-infection NAb efficacies in primary immunodeficiency virus infection.

In the present study, we examined the effect of passive NAb immunization at day 7 post-challenge on primary viral replication in a macaque AIDS model of CCR5-tropic SIVmac239 infection. Remarkably, our analysis revealed control of primary SIVmac239 replication by the passive NAb immunization post-infection.

METHODS

Animal experiments

Burmese rhesus macaques (*Macaca Mulatta*) were maintained in accordance with the Guideline for Laboratory Animals of National Institute of Infectious Diseases and National Institute of Biomedical Innovation. Major histocompatibility complex class I (MHC-I) haplotypes were determined by reference strand-mediated conformation analysis as described previously [6,26]. Blood collection, vaccination, virus challenge, passive immunization, and lymph node biopsy were performed under ketamine anesthesia. For vaccination, animals intramuscularly received a priming with 5 mg of CMV-SHIVdEN DNA encoding SIVmac239 Gag, Pol, Vif, and Vpx, SIVmac239-HIV-1_{DH12}

Academic Editor: Douglas Nixon, University of California, San Francisco, United States of America

Received May 14, 2007; **Accepted** May 23, 2007; **Published** June 20, 2007

Funding: This work was supported by a grant from the Ministry of Education, Culture, Sports, Science, and Technology, grants from the Japan Health Sciences Foundation, and grants from the Ministry of Health, Labor, and Welfare in Japan.

Competing Interests: The authors have declared that no competing interests exist.

* **To whom correspondence should be addressed.** E-mail: matano@m.u-tokyo.ac.jp.

chimeric Vpr, and HIV-1_{DH12} Tat and Rev, followed by an intranasal booster six weeks later with 1×10^8 CIU (cell infectious units) of replication-competent Sendai virus expressing Gag (SeV-Gag) in macaque V5 or 6×10^9 CIU of F-deleted replication-defective SeV-Gag in other vaccinees as described previously [6]. Animals were challenged intravenously with 1,000 $TCID_{50}$ (50 percent tissue culture infective dose) of SIVmac239, three months after booster in case of vaccinees. For passive immunization, animals were intravenously administered with 300 mg of anti-SIV immunoglobulin G (IgG) or control IgG at day 7 post-challenge.

Antibody preparation

Pools of plasma showing SIVmac239-specific NAb titers of 1:4 to 1:64 were obtained from six SIVmac239-infected rhesus macaques with NAb induction in the chronic phase for preparing the IgG inoculums for passive NAb immunization. IgG was purified from the plasma after heat-inactivation and filtration by Protein G Sepharose 4 Fast Flow (Amersham) and concentrated by Amicon Ultra 4, MW50000 (Millipore) to 30 mg/ml. This IgG solution had SIVmac239-specific NAb titer of 1:16; i.e., 5 μl of 16-fold-diluted antibodies killed 5 μl of 10 $TCID_{50}$ SIVmac239 on MT-4 cells. Control IgG was prepared from non-infected rhesus macaques. Neutralizing F(ab')2 was obtained by pepsin digestion with Immunopure F(ab')2 purification kit (Pierce).

Quantitation of plasma viral loads

Plasma RNA was extracted using High Pure Viral RNA kit (Roche Diagnostics). Serial five-fold dilutions of RNA samples were amplified in quadruplicate by reverse transcription and nested PCR using SIVmac239 *gag*-specific primers to determine the end point. Plasma SIV RNA levels were calculated according to the Reed-Muench method as described previously [6]. The lower limit of detection is approximately 4×10^2 copies/ml.

Measurement of virus-specific neutralizing titers

Serial two-fold dilutions of heat-inactivated plasma or purified antibodies were prepared in duplicate and mixed with 10 $TCID_{50}$ of SIVmac239. In each mixture, 5 μl of diluted sample was incubated with 5 μl of virus. After 45-min incubation at room temperature, each 10-μl mixture was added into 5×10^4 MT-4 cells/well in 96-well plates. Day 12 culture supernatants were harvested and progeny virus production was examined by ELISA for detection of SIV p27 core antigen (Beckman-Coulter) to determine 100% neutralizing endpoint. The lower limit of titration is 1:2.

Measurement of virus-specific T-cell responses

Virus-specific T-cell levels were measured by flow-cytometric analysis of gamma interferon (IFN-γ) induction as described previously [6]. Peripheral blood mononuclear cells (PBMCs) were cocultured with autologous herpesvirus papio-immortalized B lymphoblastoid cell lines infected with a vesicular stomatitis virus G (VSV-G)-pseudotyped SIVGP1 for SIV-specific stimulation. The pseudotyped virus was obtained by cotransfection of COS-1 cells with a VSV-G-expression plasmid and the SIVGP1 DNA, an env- and nef-deleted simian-human immunodeficiency virus (SHIV) molecular clone DNA. Intracellular IFN-γ staining was performed using CytofixCytoperm kit (Becton Dickinson). Fluorescein isothiocianate-conjugated anti-human CD4, Peridinin chlorophyll protein-conjugated anti-human CD8, allophycocyanin-conjugated anti-human CD3, and phycoerythrin-conjugated anti-human IFN-γ antibodies (Becton Dickinson) were used. Specific T-cell levels were calculated by subtracting non-specific IFN-γ^+ T-cell frequencies from those after SIV-specific stimulation. Specific T-cell levels less than 100 cells per million PBMC are considered negative.

Quantitation of cell-associated viral loads

Right and left inguinal lymph nodes and right and left axillary lymph nodes were obtained from macaques by biopsy at days 7, 8, 10, and 14 post-challenge, respectively. For measurement of dendritic cell (DC)-associated viral loads, $CD1c^+$ DCs were positively selected to over 99% purity using a macaque $CD1c^+$ DC magnetic sorting system (Miltenyi Biotech) from $CD20^-$ lymphocytes negatively-selected from lymph nodes. $CD1c^-CD20^-$ cells were used for measurement of non-DC-associated viral loads. Cell-associated viral RNA was extracted using RNeasy kit (Qiagen) and quantitated by LightCycler real-time PCR system (Roche Diagnostics) using SIV *gag*-specific primers and probes. The lower limit of detection is approximately 1,000 copies/10^6 cells.

Antigen presentation assay in vitro

PBMCs obtained in the chronic phase from SIVmac239-controllers were attached to culture plates for 4 h, and adhesive cells were cultured in the presence of 50 ng/ml GM-CSF (R&D Systems) and 5 ng/ml IL-4 (R&D Systems) for 5 days to obtain $CD1c^+CD83^+CD86^+$HLA-ABC^+HLA-DR^+ immature DCs [27]. Alternatively, $CD1c^+$ DCs were positively selected from CD20-depleted PBMCs as described above. For antigen presentation assay, 1×10^5 of the in vitro-generated DCs (Exp. 1, 2, and 3) or the positively-selected $CD1c^+$ DCs (Exp. 4) were pulsed for 17 h with 2,000 $TCID_{50}$ of SIVmac239 (corresponding to 2×10^6 SIV RNA copies and 3 ng of SIV p27) alone or preincubated for 45 min with 1.5 mg of either control IgG, neutralizing IgG, or neutralizing F(ab')2. Autologous PBMCs were cocultured with these pulsed DCs and then subjected to measurement of specific IFN-γ induction.

Statistical analysis

Statistical analysis was performed by Prism software version 4.03 (GraphPad Software, Inc.). Set point plasma viral loads and peripheral $CD95^+CD28^+$ central memory $CD4^+$ T-cell counts around 3 months after challenge of the naive controls ($n = 7$) and NAb-immunized macaques ($n = 4$) were log-transformed for improvement of normality and compared by two-tailed unpaired t test with significance levels set at $p<0.05$. Then their geometric means with 95% confidence interval were calculated. Due to the limited number of samples for each group providing difficulty for their normality testing, the two groups were additionally compared by nonparametric Mann-Whitney U test for confirmation of results. No significant difference in $CD95^+CD28^+$ central memory $CD4^+$ T-cell counts just before challenge was observed between the two groups ($p = 0.68$ by unpaired two-tailed t test with Welch's correction and $p = 0.31$ by Mann-Whitney U test) (data not shown).

RESULTS

SIV control by post-infection passive NAb immunization

While most SIVmac239-infected naive macaques usually fail to elicit NAb responses during the early phase of infection, some acquire detectable levels of NAbs against the challenge strain in the late phase. IgG purified from plasma pools of such SIVmac239-infected macaques with NAb induction, showing in

vitro SIVmac239-specific neutralizing activity of 1:16, was used for passive immunization as polyclonal anti-SIV NAbs. In the first part of this study, naive Burmese rhesus macaques were challenged intravenously with SIVmac239 followed by passive immunization with 10 ml of the polyclonal NAbs (300 mg IgG) at day 7 post-challenge (Figure 1A). Seven naive control macaques challenged with SIVmac239, including two infused with non-SIV-specific control antibodies, all failed to contain viral replication with persistent viremia (Figure 1B). These macaques showed peak plasma viral loads between days 7 and 14 post-challenge and most had set-point viral loads exceeding 1×10^4 SIV RNA copies/ml plasma. In contrast, four rhesus macaques passively immunized at day 7 with polyclonal NAbs showed significantly lower plasma viral RNA loads ($p = 0.0033$ by unpaired t test and $p = 0.0061$ by Mann-Whitney U test) compared with naive controls around 3 months post-challenge (Figures 1B&1C). Two of the NAb-immunized macaques, NA1 and NA4, controlled SIV replication with undetectable set-point plasma viremia. Thus, post-infection passive immunization of macaques with polyclonal NAbs had a significant suppressive effect on set-point viral replication.

A

NAb Tx in unvaccinated macaques

Group/macaque	Ab Tx at day 7
Naive controls	
N1*	-
N2*	-
N3*	-
N4*	-
N5	-
NC1	control Ab
NC2	control Ab

Group/macaque	Ab Tx at day 7
NAb-immunized	
NA1	anti-SIV NAb
NA2	anti-SIV NAb
NA3	anti-SIV NAb
NA4	anti-SIV NAb

B

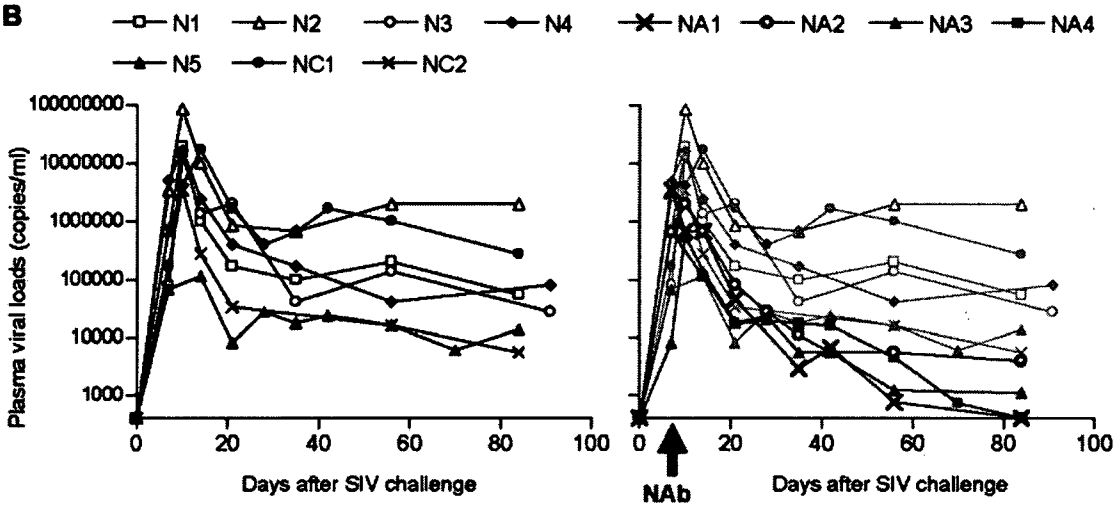

C

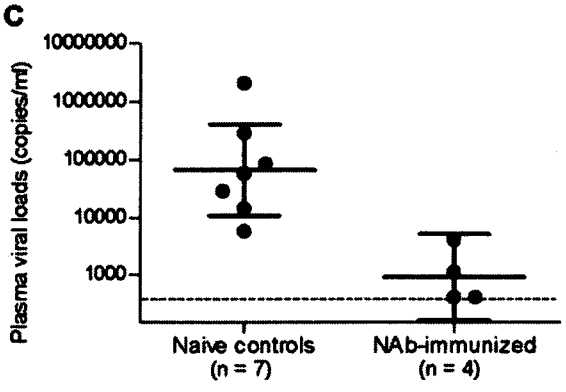

D

NAb responses

Macaque	day 7	day 10	day 14	day 35	day 84
N1	-	-	-	-	-
N2	-	-	-	-	-
N3	-	-	-	-	-
N4	-	-	-	-	-
N5	-	-	-	-	-
NC1	-	-	-	-	-
NC2	-	-	-	-	-
NA1	-	+	+	-	-
NA2	-	+	-	-	-
NA3	-	+	-	-	-
NA4	-	+	-	-	-

Figure 1. Effect of post-challenge passive NAb immunization on primary SIV infection. (A) List of naive controls and NAb-immunized macaques. Experiments using macaques indicated by asterisk have previously been performed [6]. (B) Plasma viral loads after SIVmac239 challenge (SIV RNA copies/ml). Left panel, naive controls; right panel, NAb-immunized macaques shown by red lines and naive controls by gray lines for comparison. (C) Statistical analysis of plasma viral loads around 3 months post-challenge between naive controls (n = 7) and NAb-immunized macaques (n = 4). The geometric mean (indicated by the longer bar) of viral loads in naive controls is 6.5×10^4 copies/ml, and its 95% confidence interval (indicated by the shorter bars) is $1.1\times10^4-4.0\times10^5$ copies/ml. The geometric mean in NAb-immunized macaques is 9.1×10^2 copies/ml, and its 95% confidence interval is $1.6\times10^2-5.1\times10^3$ copies/ml. The difference between the two groups was statistically significant by unpaired two-tailed t test ($p = 0.0033$) and by non-parametric Mann-Whitney U test ($p = 0.0061$). Viral loads of macaques NA1 and NA4 were calculated as the lower limit of detection shown as the dashed line (400 copies/ml). (D) Plasma NAb responses after challenge. (+), positive; (−), negative. All detected titers were no more than 1:2.
doi:10.1371/journal.pone.0000540.g001

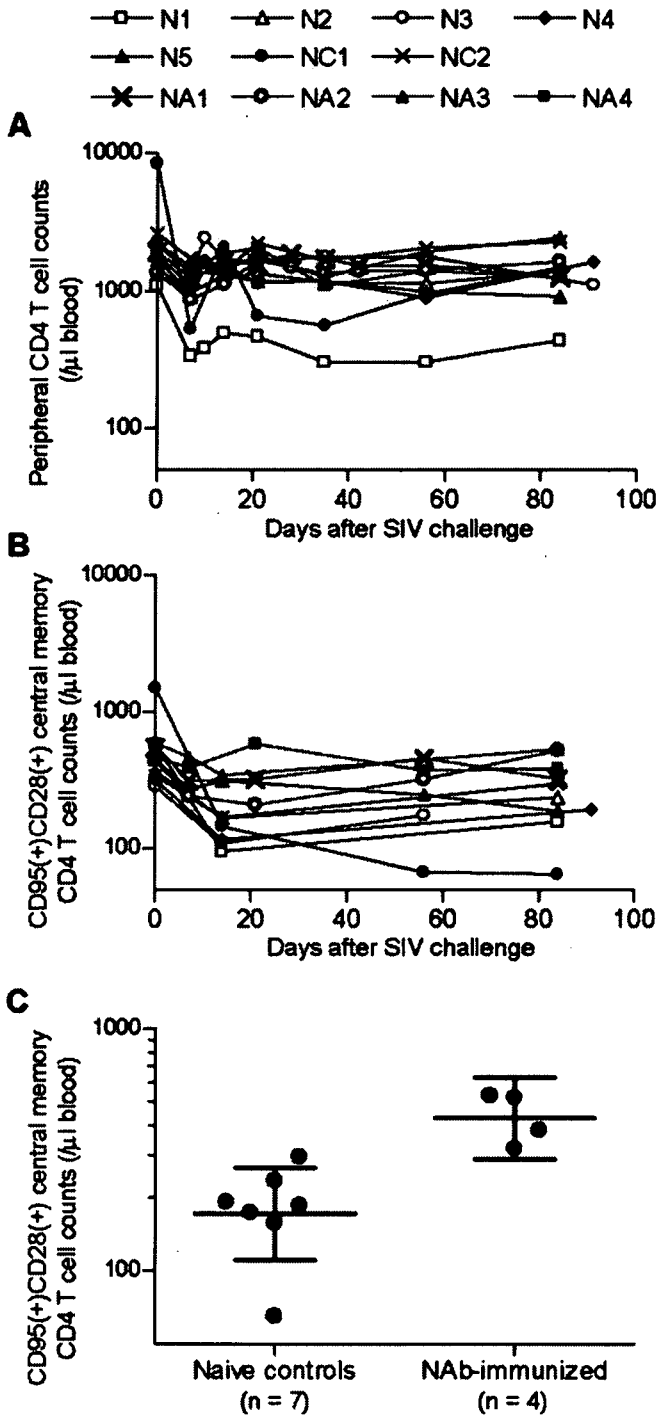

Figure 2. Central memory CD4$^+$ T-cell counts in naive controls and NAb-immunized macaques. (A) Peripheral CD4$^+$ T-cell counts (cells/μl). (B) Peripheral CD95$^+$CD28$^+$ central memory CD4$^+$ T-cell counts (cells/μl) [28]. (C) Statistical comparison of CD28$^+$CD95$^+$ central memory CD4$^+$ T-cell counts around 3 months post-challenge. The geometric mean (indicated by the longer bar) of central memory CD4$^+$ T-cell counts in naive controls is 1.7×10^2 counts/μl, and its 95% confidence interval (indicated by the shorter bars) is $1.1\times10^2-2.7\times10^2$ counts/μl. The geometric mean in NAb-immunized macaques is 4.3×10^2 counts/μl, and its 95% confidence interval is $2.9\times10^2-6.3\times10^2$ counts/μl. The difference between the two groups was statistically significant by unpaired two-tailed t test ($p=0.0066$) and by non-parametric Mann-Whitney U test ($p=0.0061$).
doi:10.1371/journal.pone.0000540.g002

Immune parameters in NAb-immunized macaques

Plasma NAb responses in the NAb-immunized macaques were detected marginally at day 10 post-infection but became undetectable within one week after the passive NAb immunization (Figure 1D), implying that the NAbs were rapidly exhausted for virus clearance. None elicited detectable *de novo* NAb responses past then. In the naive controls, no SIVmac239-specific NAbs were detected throughout the course. This discrepancy between the transient NAb detection and the persistent viremia control in the NAb-immunized macaques differed from previously-reported, dose-dependent establishment of sterile protection from CXCR4-tropic SHIV infection by pre-challenge passive NAb immunization [18–21].

Difference in total CD4$^+$ T-cell counts was not found throughout the course between the two groups (Figure 2A). Reductions in peripheral CD95$^+$ CD28$^+$ central memory CD4$^+$ T-cell counts [28–29] were observed in the naive controls after SIV challenge (Figure 2B). The NAb-immunized macaques, however, showed significantly higher central memory CD4$^+$ T-cell counts around 3 months post-challenge than those in the naive controls ($p=0.0066$ by unpaired t test and $p=0.0061$ by Mann-Whitney U test) (Figures 2B&2C), suggesting amelioration of central memory CD4$^+$ T-cell loss in the early phase of SIV infection by transient NAb responses around week 1 post-challenge. All of these NAb-immunized macaques showed efficient virus-specific CD8$^+$ T-cell induction at week 8 (Figure 3), although difference in the levels between the two groups was not significant, implying its possible enrollment in the observed viral control.

Post-infection passive NAb immunization in vaccinees

Our previous trial of a DNA-prime/SeV-Gag vector-boost vaccine in Burmese rhesus macaques has shown vaccine-based, NAb-independent control of SIVmac239 replication, suggesting association of MHC-I haplotype with this control [6,30]. We then examined possible synergy of post-challenge passive NAb immunization with the prophylactic CTL-based vaccination in suppression of SIV replication in two groups of macaques possessing MHC-I haplotype *90-088-Ij* and *90-120-Ia*, respectively (Figure 4A). In the former group of macaques possessing *90-088-Ij*, vaccinees failed to control SIV replication even after passive NAb immunization (Figure 4B). In the latter group of macaques possessing *90-120-Ia*, all 4 vaccinees without NAb immunization controlled SIVmac239 replication and had undetectable plasma viral loads after week 8 post-challenge (Figure 4B). All of them rapidly selected for a mutation escaping from $Gag_{206-216}$ epitope-specific CTL by week 5, suggesting a strong selective pressure on the virus by this CTL [6]. As for the

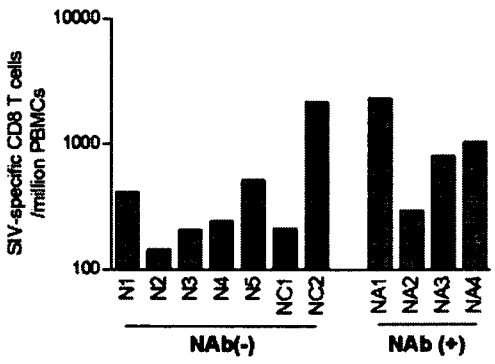

Figure 3. SIV-specific CD8$^+$ T-cell frequencies at week 8 post-challenge in naive controls and NAb-immunized macaques.
doi:10.1371/journal.pone.0000540.g003

two vaccinees VA2 and VA3 infused with NAbs, plasma viremia became undetectable by week 5 and rapid selection of CTL escape mutation was not observed (data not shown). SIV-specific $CD8^+$ T-cell frequencies at week 2 in the NAb-immunized vaccinees VA2 and VA3 were comparable with the vaccinees without NAb immunization, while SIV-specific $CD4^+$ T-cell induction at week 2 was observed in just one (V5) of the four vaccinees without NAb but in both of the NAb-immunized vaccinees (Figure 4C). These results suggest, even in the NAb-immunized vaccinees, a dominant effect of vaccine-induced cellular immune responses on control of SIV replication, although implying a possibility of NAb-mediated augmentation of CTL vaccine-based viral control.

Antibody-mediated virion uptake by DCs and T cell priming

In order to assess the possibility of altered virus distribution by NAbs, $CD1c^+$ DCs were isolated from peripheral lymph nodes of unvaccinated, SIVmac239-challenged macaques before and after passive NAb immunization, and DC-associated SIV RNA levels were quantified at the initial stage of infection. In three naive control macaques, accumulation of viral RNA to $CD1c^+$ DCs was undetectable at days 7, 8, and 10 post-challenge but became detectable at day 14 (Figure 5A). This elevation of DC-associated viral loads following peak viremia was consistent with previous immunohistochemistry reports on SIV and HIV-2 challenge experiments [31–32]. In marked contrast, both of macaques NA3 and NA4 immunized with NAbs at day 7 post-challenge showed immediate accumulation of viral RNA in $CD1c^+$ DCs at day 8 (one day after NAb immunization), suggesting antibody-mediated virion accumulation to DCs in vivo. Cell-associated viral loads in $CD1c^-CD20^-$ non-DCs were at comparable levels between the two groups, indicating that the rapid increase in DC-associated viral loads after NAb immunization was not due to changes in viral loads in lymph nodes.

Then an in vitro antigen presentation assay was performed to assume whether the early viral RNA accumulation in DCs could

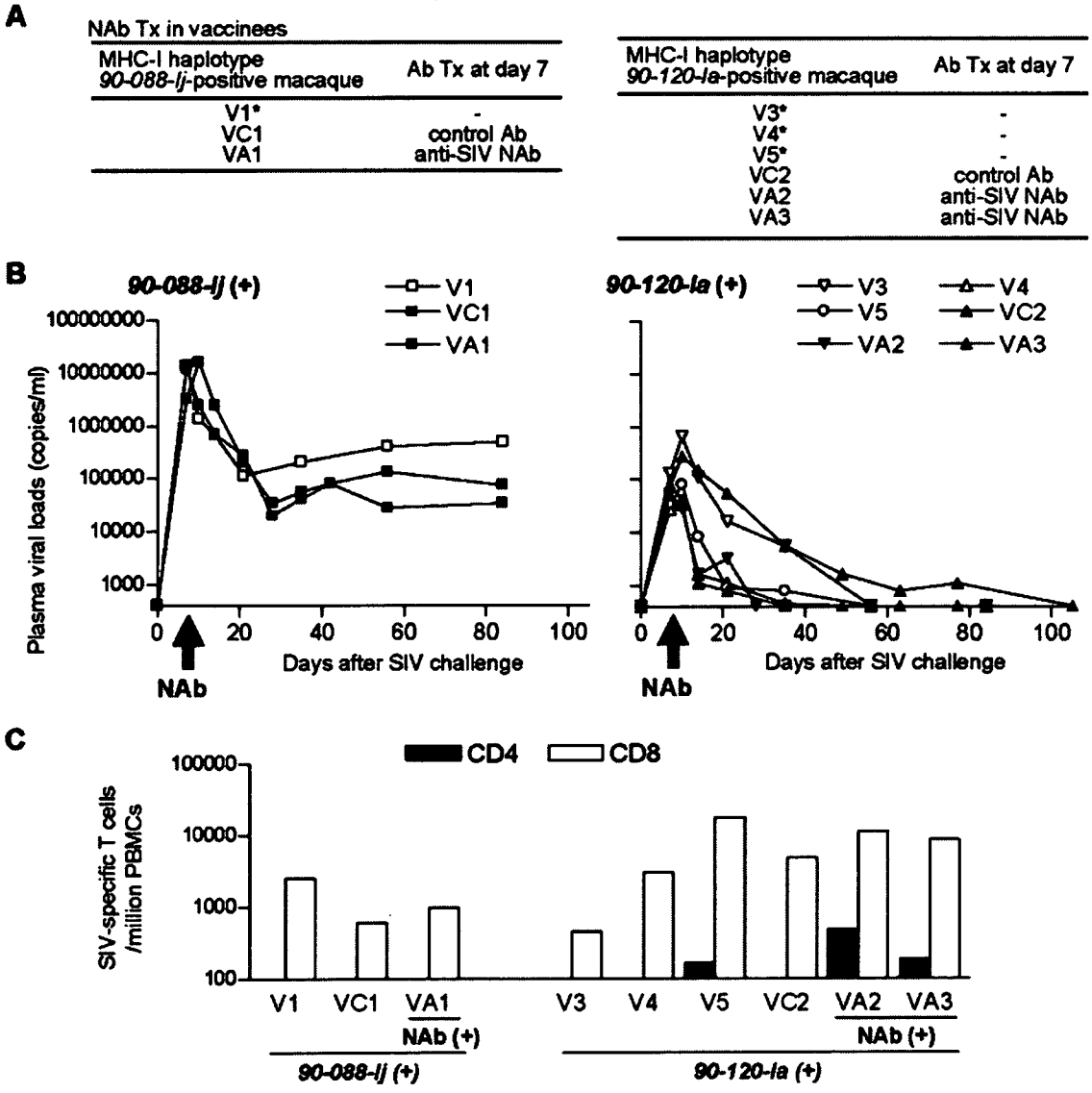

Figure 4. Effect of post-challenge passive NAb immunization in vaccinees. (A) List of vaccinees with or without passive immunization. (B) Plasma viral loads after challenge (SIV RNA copies/ml). Left panel, MHC-I haplotype *90-088-Ij*-positive macaques; right panel, *90-120-Ia*-positive macaques. Red lines represent NAb-immunized vaccinees. (C) SIV-specific $CD4^+$ T-cell and $CD8^+$ T-cell frequencies at week 2 post-challenge.
doi:10.1371/journal.pone.0000540.g004

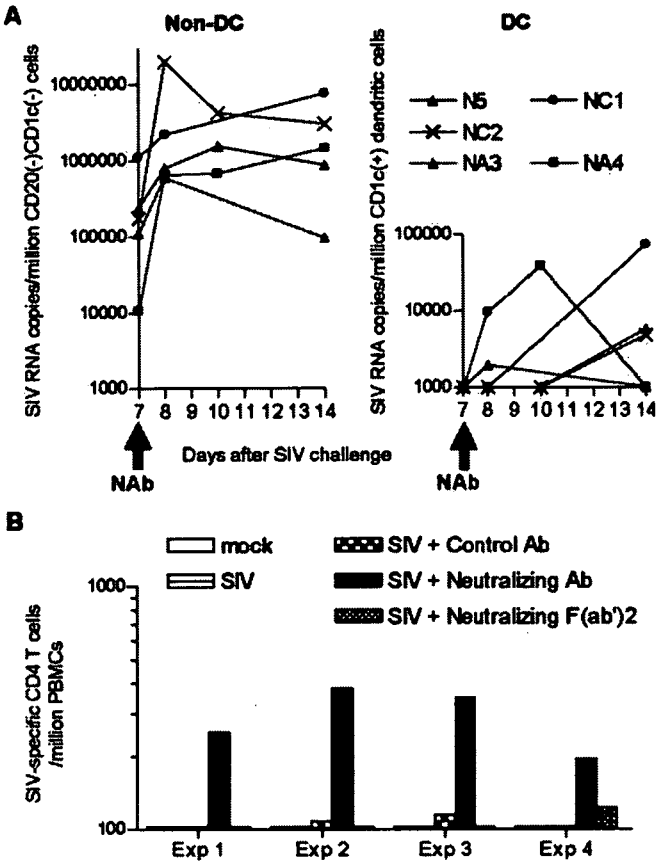

Figure 5. Antibody-mediated SIV uptake by DCs and T cell priming. (A) Peripheral lymph node-derived non-DC ($CD1c^-CD20^-$ lymphocytes)-associated (left panel) and $CD1c^+CD20^-$ DC-associated viral loads (right panel). (B) In vitro antigen presentation assay. Either in vitro-generated DCs (Exp. 1, Exp. 2, and Exp. 3) or positively-selected $CD1c^+$ DCs (Exp. 4) prepared from PBMCs were pulsed with SIV alone (SIV), SIV preincubated with control antibodies (SIV+Control Ab), SIV preincubated with NAbs (SIV+Neutralizing Ab), or SIV preincubated with Fc-depleted NAbs (SIV+Neutralizing F[ab']2). Autologous PBMCs were cocultured with these pulsed DCs and then subjected to measurement of specific IFN-γ induction.
doi:10.1371/journal.pone.0000540.g005

represent a correlation to T cell priming. DCs prepared from peripheral blood of macaques that controlled SIVmac239 replication were pulsed with antibody-neutralized SIV, and autologous PBMCs were cocultured with these pulsed DCs for measurement of specific IFN-γ induction. In all four sets of experiments, efficient IFN-γ induction in $CD4^+$ T cells was observed after stimulation by DCs pulsed with SIV preincubated with NAb but not by DCs pulsed with SIV alone, SIV preincubated with control antibodies, or SIV preincubated with Fc-depleted neutralizing F(ab')2 (Figure 5B). Efficient IFN-γ induction in $CD8^+$ T cells was not observed even after coculture with NAb-preincubated SIV-pulsed DCs except for one (Exp. 4). Overall, augmentation of virus-specific T-cell stimulation was observed by the coexistence of NAbs, suggesting their involvement in antigen presentation.

DISCUSSION

The present study showed suppression of primary SIV replication by passive NAb immunization post-infection, suggesting a possibility of HIV control by potent antibody induction during the acute phase of infection. It reversely follows that its absence may be involved in an increase in the burden of acute infectious viral loads and abrogation of virus-specific cellular immune responses, leading to initial control failure in HIV infections.

While this study does not exclude possibilities of additional antibody-mediated protective mechanisms such as antibody-dependent cell-mediated cytotoxicity or recently-reported complement virolysis [33], the non-sterile but consistent viral control at the set point by passive NAb immunization despite only transient detection of NAb responses during the acute phase coheres with involvement of cellular immune responses in this control [27,34–36]. Thus, results may provide additional interpretations to previous NAb passive immunization studies [14,16–21], which have mostly utilized CXCR4-tropic SHIV-challenged macaques and shown sterile protection by high titers of pre-challenge or very early post-challenge NAbs.

A technical confinement of this study is the use of polyclonal antibodies which may include not only NAbs but also non-neutralizing anti-SIV antibodies for passive immunization. However, our finding of primary SIV control by post-infection passive immunization with the anti-SIV inoculums with neutralizing activity presents significant evidence suggesting that potent antibodies post-infection can contribute to control of primary immunodeficiency virus infection. Whether neutralizing activity is required for the enhanced SIV control by passive immunization remains to be assessed in future studies. Our in vitro results suggest a possibility of virus-specific $CD4^+$ T-cell activation by NAbs, and neutralizing activity may contribute to protection of these virus-specific $CD4^+$ T cells from SIV *trans*-infection via DCs [37–38], possibly counteracting the abrogation of the optimal concert of adaptive immunity between $CD4^+$ T and $CD8^+$ T cells usually observed in the natural course of pathogenic immunodeficiency virus infection [23,25,39]. The possibility of failure in antibody-mediated priming of effective cellular immune responses by preexisting vaccine-induced dominant responses may account for lack of viral control in the NAb-immunized vaccinee possessing MHC-I haplotype *90-088-Ij*.

Despite suggested technical difficulties in achieving requisite neutralizing titers for sterile HIV protection by prophylactic vaccination, our results indicate a possibility of non-sterile HIV control by secondary expansion of prophylactic vaccine-induced, sub-sterile titers of NAbs post-infection, providing a rationale of vaccine-based NAb induction for primary HIV control. More understanding of the mechanism may lead to a more certain rationale for careful induction of NAbs and CTLs by vaccination, maybe potentially capable of synergistic HIV-1 control.

ACKNOWLEDGMENTS

The animal experiments were conducted through the Cooperative Research Program in Tsukuba Primate Research Center, National Institute of Biomedical Innovation with the help of the Corporation for Production and Research of Laboratory Primates. We thank DNAVEC corp. for providing Sendai virus vectors; K. Ishikawa, T. Nakasone, K. Mori, F. Ono, K. Komatsuzaki, A. Hiyaoka, H. Ogawa, K. Oto, N. Ageyama, H. Akari, and K. Terao for assistance in animal experiments; and C. Moriya, T. Tsukamoto, A. Kato, M. Miyazawa, M. Yasunami, A. Kimura, T. Sata, N. Yamamoto, T. Kurata, A. Nomoto, and Y. Nagai for their help.

Author Contributions

Conceived and designed the experiments: TM HY. Performed the experiments: TM HY MK AT HI. Analyzed the data: TM HY MK. Wrote the paper: TM HY MK. Other: Contributed to preparation of the passive immunization inoculums, experiments using DCs, and immunological analyses: HY. Contributed to immunological analyses: MK. Contributed to blood processing and immunological and virological analyses: AT. Contributed to blood processing and immunological and virological analyses: HI.

REFERENCES

1. Koup RA, Safrit JT, Cao Y, Andrews CA, McLeod G, et al. (1994) Temporal association of cellular immune responses with the initial control of viremia in primary human immunodeficiency virus type 1 syndrome. J Virol 68: 4650–4655.
2. Borrow P, Lewicki H, Hahn BH, Shaw GM, Oldstone MB (1994) Virus-specific CD8+ cytotoxic T-lymphocyte activity associated with control of viremia in primary human immunodeficiency virus type 1 infection. J Virol 68: 6103–6110.
3. Matano T, Shibata R, Siemon C, Connors M, Lane HC, et al. (1998) Administration of an anti-CD8 monoclonal antibody interferes with the clearance of chimeric simian/human immunodeficiency virus during primary infections of rhesus macaques. J Virol 72: 164–169.
4. Schmitz JE, Kuroda MJ, Santra S, Sasseville VG, Simon MA, et al. (1999) Control of viremia in simian immunodeficiency virus infection by $CD8^+$ lymphocytes. Science 283: 857–860.
5. Jin X, Bauer DE, Tuttleton SE, Lewin S, Gettie A, et al. (1999) Dramatic rise in plasma viremia after CD8(+) T cell depletion in simian immunodeficiency virus-infected macaques. J Exp Med 189: 991–998.
6. Matano T, Kobayashi M, Igarashi H, Takeda A, Nakamura H, et al. (2004) Cytotoxic T lymphocyte-based control of simian immunodeficiency virus replication in a preclinical AIDS vaccine trial. J Exp Med 199: 1709–1718.
7. Goulder PJ, Watkins DI (2004) HIV and SIV CTL escape: implications for vaccine design. Nat Rev Immunol 4: 630–640.
8. Burton DR, Desrosiers RC, Doms RW, Koff WC, Kwong PD, et al. (2004) HIV vaccine design and the neutralizing antibody problem. Nat Immunol 5: 233–236.
9. Kwong PD, Doyle ML, Casper DJ, Cicala C, Leavitt SA, et al. (2002) HIV-1 evades antibody-mediated neutralization through conformational masking of receptor-binding sites. Nature 420: 678–682.
10. Wei X, Decker JM, Wang S, Hui H, Kappes JC, Wu X, et al. (2003) Antibody neutralization and escape by HIV-1. Nature 422: 307–312.
11. Hangartner L, Zinkernagel RM, Hengartner H (2006) Antiviral antibody responses: the two extremes of a wide spectrum. Nat Rev Immunol 6: 231–243.
12. Richman DD, Wrin T, Little SJ, Petropoulos CJ (2003) Rapid evolution of the neutralizing antibody response to HIV type 1 infection. Proc Natl Acad Sci U S A 100: 4144–4149.
13. Trkola A, Kuster H, Rusert P, Joos B, Fischer M, et al. (2005) Delay of HIV-1 rebound after cessation of antiretroviral therapy through passive transfer of human neutralizing antibodies. Nat Med 11: 615–622.
14. Haigwood NL, Watson A, Sutton WF, McClure J, Lewis A, et al. (1996) Passive immune globulin therapy in the SIV/macaque model: early intervention can alter disease profile. Immunol Lett 51: 107–114.
15. Poignard P, Sabbe R, Picchio GR, Wang M, Gulizia RJ, et al. (1999) Neutralizing antibodies have limited effects on the control of established HIV-1 infection in vivo. Immunity 10: 431–438.
16. Nishimura Y, Igarashi T, Haigwood NL, Sadjadpour R, Donau OK, et al. (2003) Transfer of neutralizing IgG to macaques 6 h but not 24 h after SHIV infection confers sterilizing protection: implications for HIV-1 vaccine development. Proc Natl Acad Sci U S A 100: 15131–15136.
17. Mascola JR, Lewis MG, Stiegler G, Harris D, VanCott TC, et al. (1999) Protection of macaques against pathogenic simian/human immunodeficiency virus 89.6PD by passive transfer of neutralizing antibodies. J Virol 73: 4009–4018.
18. Shibata R, Igarashi T, Haigwood N, Buckler-White A, Ogert R, et al. (1999) Neutralizing antibody directed against the HIV-1 envelope glycoprotein can completely block HIV-1/SIV chimeric virus infections of macaque monkeys. Nat Med 5: 204–210.
19. Mascola JR, Stiegler G, VanCott TC, Katinger H, Carpenter CB, et al. (2000) Protection of macaques against vaginal transmission of a pathogenic HIV-1/SIV chimeric virus by passive infusion of neutralizing antibodies. Nat Med 6: 207–210.
20. Parren PW, Marx PA, Hessell AJ, Luckay A, Harouse J, et al. (2001) Antibody protects macaques against vaginal challenge with a pathogenic R5 simian/human immunodeficiency virus at serum levels giving complete neutralization in vitro. J Virol 75: 8340–8347.
21. Veazey RS, Shattock RJ, Pope M, Lirijan JC, Jones J, et al. (2003) Prevention of virus transmission to macaque monkeys by a vaginally applied monoclonal antibody to HIV-1 gp120. Nat Med 9: 343–346.
22. Nishimura Y, Igarashi T, Donau OK, Buckler-White A, Buckler C, et al. (2004) Highly pathogenic SHIVs and SIVs target different CD4+ T cell subsets in rhesus monkeys, explaining their divergent clinical courses. Proc Natl Aca Sci. U S A 101: 12324–12329.
23. Mattapallil JJ, Douek DC, Hill B, Nishimura Y, Martin M, et al. (2005) Massive infection and loss of memory $CD4^+$ T cells in multiple tissues during acute SIV infection. Nature 434: 1093–1097.
24. Li Q, Duan L, Estes JD, Ma ZM, Routke T, et al. (2005) Peak SIV replication in resting memory $CD4^+$ T cells depletes gut lamina propria $CD4^+$ T cells. Nature 434: 1148–1152.
25. Picker LJ, Watkins DI (2005) HIV pathogenesis: the first cut is the deepest. Nat Immunol 6: 430–432.
26. Arguello JR, Little AM, Bohan E, Goldman JM, Marsh SG, et al. (1998) High resolution HLA class I typing by reference strand-mediated conformation analysis (RSCA). Tissue Antigens 52: 57–66.
27. Sallusto F, Lanzavecchia A (1994) Efficient presentation of soluble antigen by cultured human dendritic cells is maintained by granulocyte/macrophage colony-stimulating factor plus interleukin 4 and downregulated by tumor necrosis factor alpha. J Exp Med 179: 1109–1118.
28. Pitcher CJ, Hagen SI, Walker JM, Lum R, Mitchell BL, et al. (2002) Development and homeostasis of T cell memory in rhesus macaques. J Immunol 168: 29–43.
29. Letvin NL, Mascola JR, Sun Y, Gorgone DA, Buzby AP, et al. (2006) Preserved $CD4^+$ central memory T cells and survival in vaccinated SIV-challenged monkeys. Science 312: 1530–1533.
30. Kawada M, Igarashi H, Takeda A, Tsukamoto T, Yamamoto H, et al. (2006) Involvement of multiple epitope-specific cytotoxic T-lymphocyte responses in vaccine-based control of simian immunodeficiency virus replication in rhesus macaques. J Virol 80: 1949–1958.
31. Chakrabarti L, Isola P, Cumont MC, Claessens-Maire MA, Hurtrel M, et al. (1994) Early stages of simian immunodeficiency virus infection in lymph nodes. Evidence for high viral load and successive populations of target cells. Am J Pathol 144: 1226–1237.
32. Eitner F, Cui Y, Grouard-Vogel G, Hudkins KL, Schmidt A, et al. (2000) Rapid shift from virally infected cells to germinal center-retained virus after HIV-2 infection of macaques. Am J Pathol 156: 1197–1207.
33. Huber M, Fischer M, Misselwitz B, Manrique A, Kuster H, et al. (2006) Complement lysis activity in autologous plasma is associated with lower viral loads during the acute phase of HIV-1 infection. PLoS Medicine 3: e441.
34. Regnault A, Lankar D, Lacabanne V, Rodriguez A, Thery C, et al. (1999) Fcgamma receptor-mediated induction of dendritic cell maturation and major histocompatibility complex class I-restricted antigen presentation after immune complex internalization. J Exp Med 189: 371–380.
35. Schuurhuis DH, Ioan-Facsinav A, Nagelkerken B, van Schip JJ, Sedlik C, et al. (2002) Antigen-antibody immune complexes empower dendritic cells to efficiently prime specific $CD8^+$ CTL responses *in vivo*. J Immunol 168: 2240–2246.
36. Thomas PG, Brown SA, Yue W, So J, Webby RJ, et al. (2006) An unexpected antibody response to an engineered influenza virus modifies $CD8^+$ T cell responses. Proc Natl Acad Sci U S A 103: 2764–2769.
37. Frankel SS, Steinman RM, Michael NL, Kim SR, Bhardwaj N, et al. (1998) Neutralizing monoclonal antibodies block human immunodeficiency virus type 1 infection of dendritic cells and transmission to T cells. J Virol 72: 9788–9794.
38. Lore K, Smed-Sorensen A, Vasudevan J, Mascola JR, Koup RA (2005) Myeloid and plasmacytoid dendritic cells transfer HIV-1 preferentially to antigen-specific $CD4^+$ T cells. J Exp Med 201: 2023–2033.
39. Castellino F, Germain RN (2006) Cooperation between $CD4^+$ and $CD8^+$ T cells: When, Where, and How. Annu Rev Immunol 24: 519–540.

JOURNAL OF VIROLOGY, Sept. 2007, p. 9911–9921 Vol. 81, No. 18
0022-538X/07/$08.00+0 doi:10.1128/JVI.00027-07

Defect of Human Immunodeficiency Virus Type 2 Gag Assembly in *Saccharomyces cerevisiae*▽

Yuko Morikawa,[1]* Toshiyuki Goto,[2] Daisuke Yasuoka,[1] Fumitaka Momose,[1] and Tetsuro Matano[3]

Kitasato Institute for Life Sciences and Graduate School for Infection Control, Kitasato University, Shirokane 5-9-1, Minato-ku, Tokyo 108-8641,[1] School of Health Science, Faculty of Medicine, Kyoto University, Kawahara-cho 53, Shogoin, Sakyo-ku, Kyoto 606-8507,[2] and Graduate School of Medicine, The University of Tokyo, Hongo 7-3-1, Bunkyo-ku, Tokyo 113-0033,[3] Japan

Received 5 January 2007/Accepted 25 June 2007

We have previously shown that the expression of human immunodeficiency virus type 1 (HIV-1) Gag protein in *Saccharomyces cerevisiae* spheroplasts produces Gag virus-like particles (VLPs) at the plasma membrane, indicating that yeast has all the host factors necessary for HIV-1 Gag assembly. Here we expand the study by using diverse primate lentiviral Gags and show that yeast does not support the production of HIV-2 or simian immunodeficiency virus SIVmac Gag VLPs but allows the production of SIVagm and SIVmnd Gag VLPs. Particle budding was observed at the surfaces of cells expressing SIVagm and SIVmnd Gags, but cells expressing HIV-2 and SIVmac Gags showed only membrane-ruffling structures, although they were accompanied with electron-dense submembrane layers, suggesting arrest at an early stage of particle budding. Comparison of HIV-1 and HIV-2 Gag expression revealed broadly equivalent levels of intracellular Gag expression and Gag N-terminal myristoylation in yeast. Both Gags showed the same membrane-binding ability and were incorporated into lipid raft fractions at a physiological concentration of salt. HIV-2 Gag, however, failed to form a high-order multimer and easily dissociated from the membrane, phenomena which were not observed in higher eukaryotic cells. A series of chimeric Gags between HIV-1 and HIV-2 and Gag mutants with amino acid substitutions revealed that a defined region in helix 2 of HIV-2 MA (located on the membrane-binding surface of MA) affects higher-order Gag assembly and particle production in yeast. Together, these data suggest that yeast may lack a host factor(s) for HIV-2 and SIVmac Gag assembly.

The major structural component of retroviruses is encoded by the *gag* gene, and Gag is the sole protein required for viral particle assembly. Three discrete Gag regions responsible for virus particle assembly have been identified and termed the membrane-binding (M), interacting (I), and late (L) domains. The M domain is located at the N-terminal matrix/membrane (MA) of Gag and contains a membrane-binding signal which directs the association of Gag with the membrane. The signal is largely composed of N-terminal myristoylation of MA in many mammalian retroviruses, including human immunodeficiency virus (HIV), and this modification is necessary for Gag targeting and subsequent binding to the plasma membrane (4, 14, 15). The I domain is essential for Gag-Gag interactions and spans from the central capsid (CA) to the nucleocapsid (NC) of Gag (7, 11, 24, 39). The L domain, responsible for pinching off viral particles from the membrane, is located at either the C-terminal domain of Gag or the MA-CA junction (16, 37).

Because Gag is sufficient for retroviral particle budding, many studies on particle assembly have used Gag expression and shown that expression of the Gag protein alone in higher eukaryotic cells produces a Gag virus-like particle (VLP) morphologically identical to the immature form of retroviral particles (14, 19, 44). The fact that Gag self-assembles into a viral particle suggests that Gag assembly is attributable to the intrinsic properties of Gag. This view is supported by in vitro studies in which purified Gag protein assembled into a spherical particle, analogous to a Gag VLP, in a test tube (5, 6, 22, 27). However, a number of recent studies clearly show that the Gag assembly process involves many host factors, some of which are indispensable for particle budding. These include endosomal sorting molecules, such as TSG101, Nedd4, AIP-1/ALIX, and AP-3 (9, 12, 46, 52, 53). Such host factors and protein sorting pathways appear to be commonly used machinery for intracellular trafficking of diverse retroviral Gags (21, 53). ABCE1/HP68 has also been identified as a host factor that supports multimerization of all primate lentiviral Gags (10, 56). In contrast, the host factors identified as host restriction factors, such as cyclophilin A and TRIM-5α, appear to be Gag type specific, although they are not involved in particle assembly but in uncoating and initiation of reverse transcription (2, 3, 20, 47, 50).

Recent studies on reverse genetics use small interfering RNAs, which specifically silence the expression of their corresponding genes. This new technology has made it possible to deplete a host factor of interest in mammalian cells. The study of genetics in eukaryotes has long been carried out with *Saccharomyces cerevisiae*, because yeast has the ability to replace the wild-type chromosomal copy of a gene with a mutant or deletion derivative, a property which is not available in other eukaryotic cells. Accordingly, many genetic mutants have been isolated in yeast and made available for the study of cellular factors and machinery. We previously developed a Gag VLP budding system with *Saccharomyces cerevisiae* in which the

* Corresponding author. Mailing address: Kitasato Institute for Life Sciences and Graduate School for Infection Control, Kitasato University, Shirokane 5-9-1, Minato-ku, Tokyo 108-8641, Japan. Phone: 81-3-5791-6129. Fax: 81-3-5791-6268. E-mail: morikawa@lisci.kitasato-u.ac.jp.

▽ Published ahead of print on 3 July 2007.

HIV type 1 (HIV-1) Gag protein simultaneously budded Gag VLPs from the plasma membrane, and we have suggested that a combination of this method and yeast genetics may be a powerful tool for the study of the host factors required for particle production (42). Here we expand this study by using diverse primate lentiviral Gags and show that yeast does not support the production of HIV-2 or simian immunodeficiency virus SIVmac Gag VLPs. Our data suggest that yeast may lack a host factor(s) required for tight membrane binding of HIV-2 Gag to facilitate higher-order assembly.

MATERIALS AND METHODS

Construction and expression of diverse primate lentivirus *gag* genes. For expression in yeast, the full-length *gag* genes of HIV-1 (HXB2 strain), HIV-2 (ROD strain), SIVmac (mac239 strain), SIVagm (TYU1 strain), and SIVmnd (GB1 strain) were amplified by PCRs using relevant forward and reverse primers. For the Gag-Flag fusion protein, the *gag* gene (truncated just before the termination codon) was amplified by PCR using a reverse primer containing a Flag epitope tag sequence. DNA construction of chimeric Gags between HIV-1 and HIV-2 and of Gag mutants containing amino acid substitutions was also carried out by PCRs using the relevant forward and reverse primers. The PCR fragments were cloned into the yeast expression vector pKT10 (48), which is a 2μm plasmid containing the *URA3* gene as a selective marker and the constitutive promoter for the yeast glyceraldehyde-3-phosphate dehydrogenase gene. The *S. cerevisiae* strain RAY3A-D (*MAT*a/α *ura3/ura3 his3/his3 leu2/leu2 trp1/trp1*) (40) was transformed with the yeast expression plasmids.

For expression in higher eukaryotic cells, the *gag* genes of HIV-1 and HIV-2 were modified C-terminally with a Flag epitope tag and cloned into the higher eukaryotic expression vector pCAGGS (30), which contains the promoter for the actin gene. The codon usage of the HIV-1 *gag* gene was optimized. HeLa and 293T cells were transfected with the expression plasmids by using Lipofectamine 2000 (Invitrogen).

Preparation of yeast spheroplasts and subcellular fractionation. The procedure for yeast spheroplast formation was described previously (39). In brief, yeast transformants were grown at 30°C in synthetic defined medium without uracil (0.67% yeast nitrogen base, 2% glucose, and amino acid mixtures without uracil). Yeast cells were suspended in wash buffer (50 mM Tris [pH 7.5], 5 mM $MgCl_2$, and 1 M sorbitol) containing 30 mM dithiothreitol (DTT) and incubated at 30°C for 20 min with gentle shaking. The cells were resuspended in wash buffer containing 3 mM DTT and 0.4 mg/ml Zymolyase and incubated at 30°C for 20 min with gentle shaking for digestion of the cell wall. Following digestion, the cells were washed with 1 M sorbitol.

Subcellular fractionation of yeast cells was performed by a standard procedure (13). Yeast spheroplasts (10 optical density [OD] units) were resuspended in buffer (50 mM Tris [pH 8.0], 1 mM EDTA, 1 mM DTT, 1 mM phenylmethylsulfonyl fluoride, and 1 μg/ml pepstatin A), with 150 mM NaCl or without salt, and homogenized with 15 strokes in a homogenizer. Following clarification at 500 × *g* for 5 min at 4°C, the cell lysates (whole-cell lysates) were subjected to centrifugation at 13,000 × *g* for 10 min at 4°C. The precipitates were stored as P13 fractions. The supernatants were centrifuged in a TLA100 rotor (Beckman Coulter) at 100,000 × *g* for 1 h at 4°C, and the precipitates (P100) and supernatants (S100) were separated.

Sedimentation analysis. Whole-cell lysates and subcellular fractions were applied to 20 to 70% (wt/vol) sucrose gradients in phosphate-buffered saline (PBS) and sedimented in an SW55 rotor at 120,000 × *g* for 2 h at 4°C, as described previously (28). Fractions of the gradients were collected and subjected to sodium dodecyl sulfate-polyacrylamide gel electrophoresis (SDS-PAGE) followed by Western blotting. The 80S ribosome and the immature form of HIV Gag VLPs purified from Gag-expressing HeLa cells were used as molecular weight markers for sedimentation analysis.

Membrane and lipid raft flotation centrifugation. Equilibrium flotation centrifugation with membranes was performed as described previously (32, 36), with minor modifications. The formation of yeast spheroplasts was carried out as described above. Yeast spheroplasts (10 OD units) were resuspended in buffer A (50 mM Tris [pH 8.0], 1 mM EDTA, 1 mM DTT, 1 mM phenylmethylsulfonyl fluoride, and 1 μg/ml pepstatin A) containing 150 mM NaCl. Following a brief sonication, the cell lysates were clarified at 500 × *g* for 5 min at 4°C. The supernatants were adjusted to 70% (wt/vol) sucrose in PBS, layered at the bottom of 70%-65%-10% (wt/vol) sucrose step gradients in PBS, and subjected to equilibrium flotation centrifugation. Centrifugation was performed in an SW55 rotor (Beckman Coulter) at 4°C at 120,000 × *g* overnight. In some experiments, cells were resuspended in buffer A with 500 mM NaCl or without salt. For lipid raft flotation, the cell lysates, after sonication, were treated on ice with 0.5% Triton X-100 for 10 min. Following clarification, the supernatants were subjected to equilibrium flotation centrifugation. Fractions of the gradients were collected and subjected to SDS-PAGE followed by Western blotting. Membranes of higher eukaryotic cells were analyzed similarly by equilibrium flotation centrifugation.

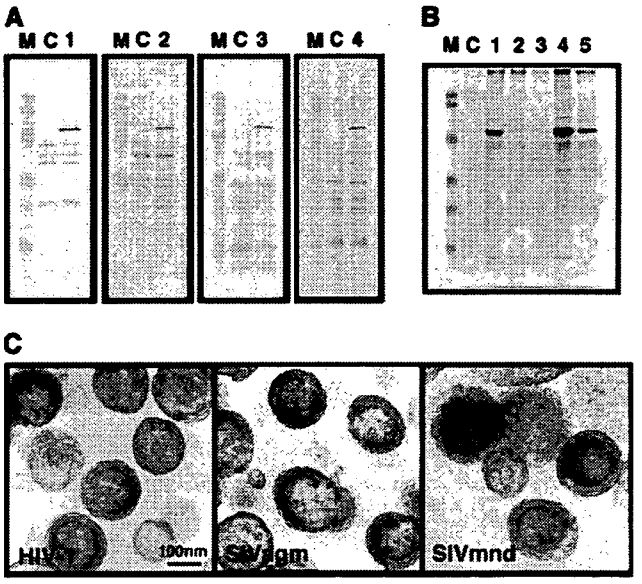

FIG. 1. Intracellular expression of diverse lentiviral Gags and production of Gag VLPs in yeast. Yeast cells were transformed with a pKT10 vector containing the full-length *gag* gene of HIV-1, HIV-2, SIVmac, SIVagm, or SIVmnd. (A) Intracellular Gag expression. Cells (0.5 OD unit) were subjected to SDS-PAGE followed by Western blotting using anti-HIV-1, anti-HIV-2, or anti-SIVmac CA antibody or anti-SIVagm monkey serum. Lanes: M, prestained molecular weight markers; C, cells transformed with the parental vector; 1 to 4, cells transformed with the vector containing the *gag* genes of HIV-1, HIV-2, SIVmac, and SIVagm, respectively. (B) Gag VLP production. Following removal of the cell wall, spheroplasts (200 OD units) were cultured in yeast extract-peptone-dextrose medium containing 1 M sorbitol overnight. Gag VLPs were purified from the culture medium by centrifugation on 20 to 70% sucrose gradients and analyzed by SDS-PAGE followed by CBB staining. Lanes: M, prestained molecular weight markers; C, mock fractions prepared from the culture medium of yeast spheroplasts transformed with the parental vector; 1 to 5, Gag VLP fractions purified from culture medium of yeast spheroplasts expressing HIV-1, HIV-2, SIVmac, SIVagm, and SIVmnd Gags, respectively. (C) Electron micrographs of Gag VLPs. Purified Gag VLP fractions were subjected to electron microscopic analysis. All micrographs are shown at the same magnification. Bar = 100 nm.

Purification of Gag VLPs. Purification of yeast-produced Gag VLPs was carried out as described previously (42). Briefly, the culture medium of yeast spheroplasts was clarified and then centrifuged through 30% (wt/vol) sucrose cushions in an SW28 rotor (Beckman Coulter) at 120,000 × *g* for 1.5 h at 4°C. The VLP pellets were resuspended and centrifuged in 20 to 70% (wt/vol) sucrose gradients in PBS in an SW55 rotor (Beckman Coulter) at 120,000 × *g* overnight at 4°C. Purification of Gag VLPs produced by higher eukaryotic cells was carried out by standard procedures.

Protein detection. Following SDS-PAGE, gels were subjected to either Coomassie brilliant blue (CBB) staining or Western blotting using an anti-HIV-1, anti-HIV-2, or anti-SIVmac CA mouse monoclonal antibody (Advanced Biotechnologies) or anti-SIVagm monkey serum. For the Gag-Flag fusion protein, Western blotting was carried out using an anti-Flag mouse monoclonal antibody (Sigma). In subcellular fractionation experiments, anti-Pep12 (for endosomes), anti-alkaline phosphatase (for vacuoles), and anti-phosphoglycerate kinase (for cytosol) mouse monoclonal antibodies (Molecular Probes) were used as or-

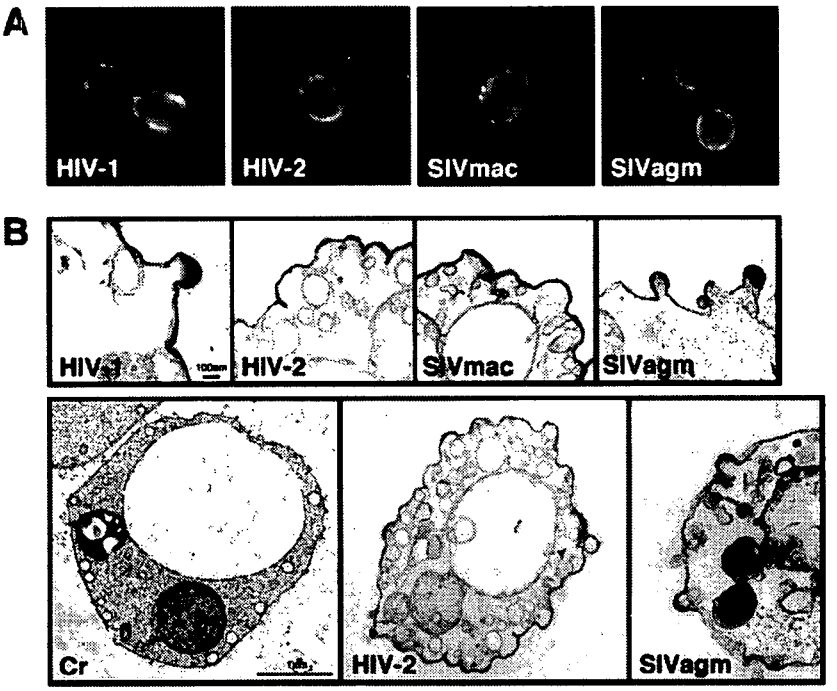

FIG. 2. Immunofluorescence staining and electron microscopy of yeast cells expressing diverse lentiviral Gags. (A) Immunofluorescence detection of Gag antigens. After fixation with 3.7% formalin, the cell wall was removed with Zymolyase and the membrane was permeabilized with 0.1% Triton X-100. Gag antigens were detected using anti-HIV-1, anti-HIV-2, or anti-SIVmac CA antibody or anti-SIVagm monkey serum. (B) Electron micrographs of yeast spheroplasts expressing each of the Gags. Micrographs in upper panels are shown at the same magnification (bar = 100 nm). Micrographs in lower panels show whole yeast cells taken at the same magnification (bar = 1 μm). Cr, yeast cell transformed with the parental vector.

ganelle markers. For the plasma membrane, yeast spheroplasts were incubated with cholera toxin subunit B (CTB), which binds to lipid rafts of the plasma membrane, at 4°C. Following a wash with 1 M sorbitol, subcellular fractionation was carried out as described above. The fractions were subjected to Western blotting using anti-CTB rabbit antibody (Molecular Probes).

For protein myristoylation, yeast cells were metabolically labeled with 500 μCi of [9,10(*n*)-^{3}H]myristic acid at 30°C for 30 min. Following SDS-PAGE, gels were subjected to fluorography.

Immunofluorescence staining. Yeast cells were fixed in 3.7% formalin in yeast extract-peptone-dextrose medium at 30°C for 30 min. Following removal of the cell wall, spheroplasts were treated with 0.1% Triton X-100 at room temperature for 5 min for membrane permeabilization. The cells were incubated first with an anti-HIV-1, anti-HIV-2, or anti-SIVmac CA mouse monoclonal antibody (Advanced Biotechnologies) or anti-SIVagm monkey serum and subsequently with anti-mouse immunoglobulin G–Alexa Fluor 488 (Molecular Probes) or anti-monkey immunoglobulin G–fluorescein isothiocyanate. For the Gag-Flag fusion protein, cells were incubated with an anti-Flag mouse monoclonal antibody (Sigma). For the plasma membrane, yeast spheroplasts were first incubated with CTB at 4°C (to label lipid rafts of the plasma membrane but not allow endocytosis) and subsequently with anti-CTB rabbit antibody (Vyrant lipid raft labeling kit; Molecular Probes). After fixation with 3.7% formalin, the spheroplasts were permeabilized with 0.1% Triton X-100 and costained with anti-Flag antibody for Gag-Flag.

Electron microscopy. Electron microscopy was carried out by standard procedures. Briefly, yeast spheroplasts were fixed in 2% glutaraldehyde in 50 mM cacodylate buffer (pH 7.2) for 2 h and postfixed with 1% osmium tetroxide for 1 h. Cell pellets were embedded in epoxy resin. Ultrathin sections were stained with uranyl acetate and lead citrate and examined with an electron microscope.

RESULTS

Yeast does not support HIV-2 or SIVmac Gag VLP production. The initial goal of this study was to examine whether Gag proteins of diverse primate lentiviruses produce Gag VLPs from yeast spheroplasts, as does HIV-1 Gag (42). Primate lentiviruses are classified into the following five equidistant phylogenetic lineages: (i) HIV-1/SIVcpz, (ii) HIV-2/SIVmac/SIVsm, (iii) SIVagm, (iv) SIVmnd, and (v) SIVsyk (17). We used the *gag* genes from four different primate lentivirus lineages. Yeast cells were transformed with the yeast expression vector pKT10 containing the *gag* gene of HIV-1, HIV-2, SIVmac, SIVagm, or SIVmnd and were grown in synthetic defined medium without uracil. Western blotting using anti-HIV-1, anti-HIV-2, and anti-SIVmac CA antibodies and anti-SIVagm monkey serum revealed individual Gag proteins in the expressing cells but not in the cells transformed with a parental vector (Fig. 1A). We did not test the cells expressing SIVmnd Gag because an anti-SIVmnd antibody was not available.

Following removal of the cell wall, yeast spheroplasts were maintained under isotonic conditions overnight. For purification of Gag VLPs, the culture medium of the spheroplasts was subjected to centrifugation through a sucrose gradient and subsequent fractionation, as described previously (42). When equivalent volumes of the Gag VLP fractions were subjected to SDS-PAGE followed by CBB staining, Gag VLP production was observed for HIV-1, SIVagm, and SIVmnd Gags, although the yields of produced VLPs varied. In contrast, no Gag VLP production was observed for HIV-2 or SIVmac Gag (Fig. 1B). Western blotting using anti-HIV-2 and anti-SIVmac CA antibodies also failed to demonstrate Gag VLP production (data not shown). These findings were not specific to the yeast expression vectors or yeast backgrounds used (data not shown).

Electron microscopic analysis confirmed that the produced SIVagm and SIVmnd Gag VLPs were nearly spherical, with electron-dense submembrane layers, similar to HIV-1 Gag VLPs prepared from yeast in parallel (Fig. 1C). The electron-dense submembrane layers, however, were often crescent-shaped or composed of multidomains.

Expression of HIV-2 and SIVmac Gags in yeast causes plasma membrane ruffling but no particle budding. We carried out an immunofluorescence study and examined the intracellular localization of each Gag protein. Microscopy revealed that all Gags tested (HIV-1, HIV-2, SIVmac, and SIVagm Gags) were localized predominantly in proximity to the plasma membrane (Fig. 2A). The data suggest that HIV-2 and SIVmac Gags are capable of targeting the plasma membrane in yeast, as are HIV-1 and SIVagm Gags. These findings were later confirmed by experiments in which Gags were costained with lipid rafts of the plasma membrane (Fig. 3C).

Electron microscopic analysis was carried out to examine whether Gag VLPs budded from the cell surfaces of the spheroplasts (Fig. 2B). Consistent with the results of our previous study (42), the spheroplasts expressing HIV-1 Gag showed half-spherical budding structures with electron-dense submembrane layers on the plasma membrane. A similar morphology was observed for cells expressing SIVagm Gag. In contrast, the spheroplasts expressing HIV-2 and SIVmac Gags revealed plasma membrane ruffling but no budding particle with a pinch or a thin stalk (Fig. 2B, top panels). The ruffling membrane, especially the area with outward curvature, had an electron-dense submembrane layer, suggesting that Gag proteins were gathered and budded but soon arrested at a very early stage of particle budding (Fig. 2B, top and lower middle panels). A yeast spheroplast characteristic of HIV-2 Gag expression is shown in Fig. 2B (lower middle panel). Nearly all the cells observed had plasma membrane ruffling that, in many cases, extended to a broad area of the plasma membrane. This finding was not observed for cells transformed with a parental vector (Fig. 2B, lower left panel) or for cells expressing SIVagm Gag (Fig. 2B, lower right panel).

Expression, N-terminal myristoylation, and plasma membrane targeting of HIV-2 Gag are comparable to those of HIV-1 Gag in yeast. Since HIV-2 and SIVmac fall into the same primate lentivirus lineage, HIV-2 was chosen and compared with HIV-1. We noticed that the sensitivity of the anti-HIV-2 CA antibody used was much lower than that of the anti-HIV-1 CA antibody (data not shown). For normalization, both Gag proteins were modified by adding a Flag epitope tag at the C terminus and were detected by an anti-Flag antibody. Expression of the Gags in yeast and VLP production were carried out as described above. Western blotting using anti-Flag antibody confirmed that no Gag VLP production was observed for HIV-2 Gag, despite the nearly equivalent levels of Gag expression in the cells (Fig. 3A). These data indicate that yeast essentially does not support HIV-2 Gag VLP production.

Because the failure was not due to a low level of HIV-2 Gag expression in yeast, we next examined the levels of Gag N-terminal myristoylation. Yeast cells were metabolically labeled with [9,10(n)-^{3}H]myristic acid and subjected to SDS-PAGE followed by fluorography. In both cases, one major radiolabeled band was detected at a gel position identical to that of the band detected by Western blotting probed with anti-CA

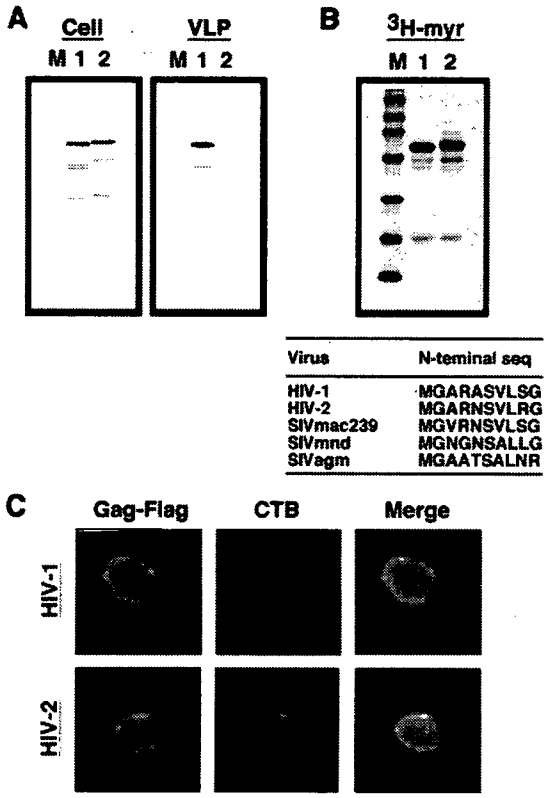

FIG. 3. N-terminal myristoylation, plasma membrane targeting, and VLP production of HIV-1 and HIV-2 Gags. Yeast cells were transformed with a pKT10 vector containing the HIV-1 or HIV-2 *gag* gene with a Flag epitope sequence added at the C terminus. (A) Intracellular Gag expression and Gag VLP production. Preparation of samples was carried out as described in the legend for Fig. 1. SDS-PAGE was followed by Western blotting using anti-Flag antibody. Lanes: M, prestained molecular weight markers; 1 and 2, expression of HIV-1 and HIV-2 Gag-Flag, respectively. (B) N-terminal myristoylation of Gag. HIV-1 and HIV-2 Gag-Flag proteins were metabolically labeled with [^{3}H]myristic acid in yeast and subjected to SDS-PAGE. Lanes: M, ^{14}C-labeled molecular weight markers; 1 and 2, cells expressing HIV-1 and HIV-2 Gag-Flag, respectively. (C) Intracellular distribution of Gag. Yeast spheroplasts expressing HIV-1 and HIV-2 Gag-Flag were incubated with CTB and then anti-CTB antibody at 4°C (not to allow endocytosis) (shown in red). After fixation with 3.7% formalin, the spheroplasts were permeabilized with 0.1% Triton X-100 and costained with anti-Flag antibody (shown in green).

antibody. The data clearly showed that the efficiencies of ^{3}H incorporation were comparable between the two Gags, indicating that both Gags were equally myristoylated in yeast (Fig. 3B). A protein myristoylation signal lies on the eight N-terminal amino acid residues (51), and the N-terminal amino acid sequences are well conserved between HIV-1 and HIV-2 Gags (Fig. 3B).

We observed that both Gags similarly localized in proximity to the plasma membrane (Fig. 2A). To confirm the plasma membrane targeting, lipid rafts of the yeast plasma membrane were probed with CTB and Gag-Flag was costained with anti-Flag antibody, as recent studies have identified the presence of lipid rafts in the yeast membrane (1). Microscopy revealed that HIV-1 Gag-Flag localized on the cell periphery, with partial colocalization with lipid rafts on the plasma membrane. Similar

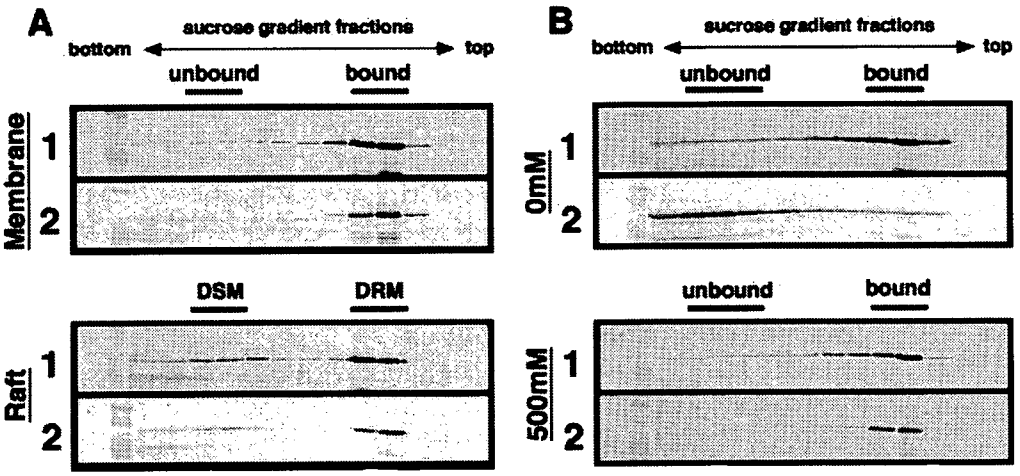

FIG. 4. Membrane and lipid raft associations of HIV-1 and HIV-2 Gags in yeast. Protein expression in yeast was carried out as described in the legend for Fig. 3. Panels: 1, cells expressing HIV-1 Gag-Flag; 2, cells expressing HIV-2 Gag-Flag. (A) Membrane and lipid raft associations of Gags at a physiological concentration of salt. Following formation of spheroplasts, cells (10 OD units) were resuspended in buffer with 150 mM NaCl and disrupted by sonication. For analysis of lipid raft association, the cell lysate was treated on ice with 0.5% Triton X-100 for 10 min. The cell lysate was clarified by low-speed centrifugation and subjected to equilibrium flotation centrifugation using a 70%-65%-10% (wt/vol) sucrose step gradient. The gradient fractions were collected from the bottom to the top (left to right) and analyzed by Western blotting using anti-Flag antibody. DSM, detergent-sensitive membrane; DRM, detergent-resistant membrane. (B) Membrane affinity of Gag in the absence of salt or under high-salt conditions. Spheroplasts (10 OD units) were resuspended in buffer, with or without 500 mM NaCl, and disrupted by sonication. After clarification by brief centrifugation, the cell lysate was subjected to equilibrium flotation centrifugation as described above.

findings were observed for HIV-2 Gag-Flag, indicating that both Gags were capable of being targeted to the plasma membrane in yeast (Fig. 3C).

HIV-2 Gag dissociates from yeast membrane in the absence of salt. To test the membrane-binding ability of Gag, membrane flotation experiments were carried out using sucrose step gradients. The initial analysis was performed at a physiological concentration of salt (150 mM NaCl). When cells expressing HIV-1 Gag-Flag were analyzed, Gag was detected in the interface fractions between the 10% and 65% sucrose layers. A similar flotation profile was observed for HIV-2 Gag-Flag, indicating that both Gags efficiently bound to the yeast membrane (Fig. 4A, top panels). It has been shown that lipid rafts are membrane microdomains that are insoluble by nonionic detergents and function as a platform for particle assembly and budding (29, 33). A similar detergent insensitivity has been reported for lipid rafts of yeast (1). Thus, Gag association with yeast lipid rafts was examined by similar equilibrium flotation centrifugation, but after a 0.5% Triton X-100 treatment on ice. When cells expressing HIV-1 Gag-Flag were analyzed, the majority of Gag was distributed in the detergent-resistant membrane fractions, suggesting that a relatively large population of the membrane-bound Gag was incorporated into the raft fractions. Very similar findings were observed for HIV-2 Gag-Flag (Fig. 4A, bottom panels). These data indicate that the two Gags show equal membrane-binding abilities and incorporation into lipid raft fractions in yeast.

However, when the sample preparation was carried out in the absence of salt and subjected to membrane flotation analysis, a striking difference was observed between the behaviors of HIV-1 and HIV-2 Gags: HIV-1 Gag displayed membrane binding, but HIV-2 Gag did not (Fig. 4B, top panels). In contrast, no differences were observed when the samples were prepared under high-salt conditions (Fig. 4B, bottom panels). These results suggest that although both Gags bind efficiently to the yeast membrane, HIV-2 Gag more readily dissociates in the absence of salt than does HIV-1 Gag.

HIV-2 Gag fails to form high-order multimers in yeast. The Gag distribution in yeast was also examined by subcellular fractionation experiments. A differential sedimentation procedure (13) yielded P13, P100, and S100 fractions, and the fractions were probed for organelle markers by Western blotting. Consistent with previous reports (13), alkaline phosphatase (for vacuoles) was found in the P13 fraction, while Pep12 (for endosomes) was found predominantly in the P100 fraction. Phosphoglycerate kinase is an abundant cytosolic protein and therefore was localized to the S100 fraction. The CTB bound to lipid rafts of the spheroplast surfaces was found in the P13 fraction (Fig. 5A, left panel). When fractions were prepared at a physiological concentration of salt (150 mM NaCl) and subjected to Western blotting, for both Gags the majority of Gag was observed in the P13 and P100 fractions, indicating that HIV-2 Gag similarly associated with the yeast membrane. However, when the fractionation was carried out in the absence of salt, the Gag distributions differed. The HIV-2 Gag shifted predominantly to the S100 fraction, while in contrast, HIV-1 Gag was detected in the same fractions as those observed in the presence of salt, confirming that HIV-2 Gag easily dissociated from the yeast membrane in the presence of salt (Fig. 5A, right panel).

To further understand these phenomena, the subcellular fractions were subjected to sedimentation analysis on 20 to 70% sucrose gradients and Gag antigens spread within the gradients were detected by Western blotting (Fig. 5B). The initial analysis was performed using the samples prepared in the absence of salt (Fig. 5B, right panels). When the whole-cell lysate from yeast expressing HIV-1 Gag was analyzed, Gag antigens were found in the 25 to 30% and 50% sucrose frac-

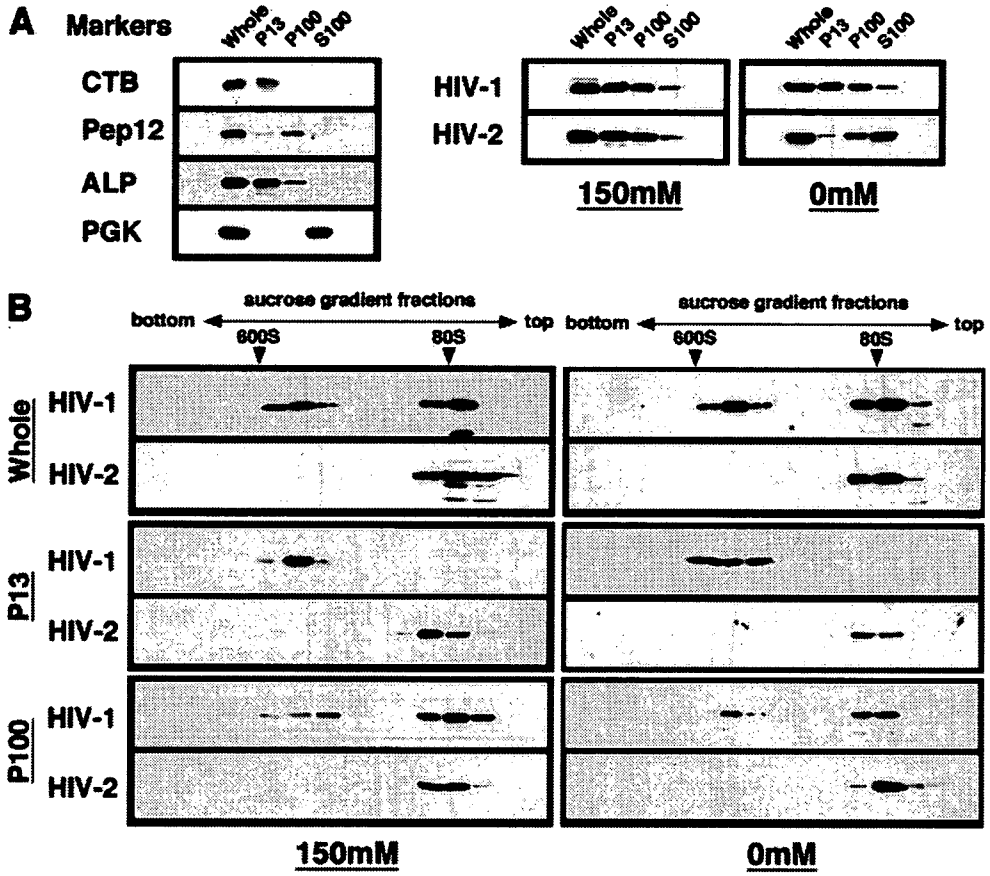

FIG. 5. Subcellular fractionation of yeast and sedimentation analysis of HIV-1 and HIV-2 Gags. Protein expression in yeast was carried out as described in the legend for Fig. 3. Following the formation of spheroplasts, cells (10 OD units) were resuspended in buffer with or without salt. (A) Subcellular fractionation. Subcellular fractionation was carried out in the presence or absence of salt, and Gag distribution was monitored by Western blotting using anti-Flag antibody (right panels). Subcellular fractions were probed for the following organelle markers: CTB (for lipid rafts on the plasma membrane), Pep12 (for endosomes), alkaline phosphatase (ALP) (for vacuoles), and phosphoglycerate kinase (PGK) (for cytosol) (left panel). (B) Sedimentation analysis of Gag. The whole-cell lysate and subcellular fractions were analyzed on 20 to 70% sucrose gradients by centrifugation at 120,000 × *g* for 2 h, and gradient fractions were subjected to Western blotting using anti-Flag antibody. Arrowheads show sedimented positions of the immature form of HIV capsid (600S) and of 80S ribosomes.

tions, likely corresponding to relatively small- and large-molecular-weight complexes, respectively. In contrast, sedimentation analysis using the whole-cell lysate from yeast expressing HIV-2 Gag revealed the presence of a Gag complex in the 25 to 30% sucrose fractions, but no other larger classes of Gag complex were seen. For more physiological conditions, we prepared the whole-cell lysate in the presence of 150 mM NaCl and carried out sedimentation analysis (Fig. 5B, left panels). The sedimentation profiles were essentially similar to those of the samples prepared in the absence of salt. These data indicate that HIV-2 Gag does not form high-order Gag multimers in yeast, although it cannot be ruled out that sedimentation analysis through 20 to 70% sucrose gradients might lead to dissociation of high-order assembly of HIV-2 Gag. The P13 and P100 fractions were also subjected to sedimentation analysis. In the case of HIV-1 Gag, the P13 fractions included predominantly the higher-order Gag multimers, while the P100 fractions included both high- and low-order Gag multimers, suggesting, though not proving, higher-order Gag assembly at the plasma membrane rather than at the endosome fractions. As expected, no high-order HIV-2 Gag multimers were detected in the P13 or P100 fraction.

Both HIV-1 and HIV-2 Gags efficiently associate with the mammalian cell membrane and form high-order multimers. For comparison, we expressed HIV-1 and HIV-2 Gag-Flag in higher eukaryotic cells, such as HeLa and 293T cells. Intracellular expression and particle production were examined by Western blotting using anti-Flag antibody. The expression levels in the cells were broadly comparable, and the production of HIV-2 particles was not impaired in either HeLa or 293T cells (Fig. 6A). Consistent with these results, when the membrane-binding affinities of Gags in the absence of salt were analyzed by membrane flotation centrifugation, the majority of Gag was found in membrane-bound fractions for both Gag types (Fig. 6B). Furthermore, when the whole-cell lysate was prepared in the absence of salt and subjected to sedimentation analysis on 20 to 70% sucrose gradients, high-order Gag multimers which sedimented in the 50% sucrose fractions were observed for both Gag types (Fig. 6C). Together, these results indicate that HIV-2 Gag, similar to HIV-1 Gag, bound efficiently to the cell

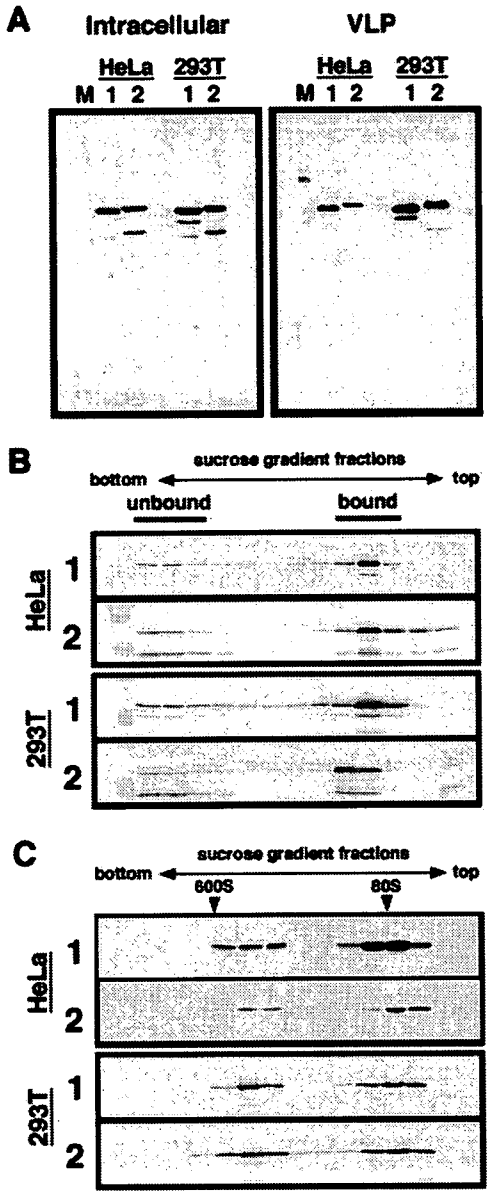

FIG. 6. Membrane association and multimerization of HIV-1 and HIV-2 Gags in higher eukaryotic cells. HeLa and 293T cells were transfected with a pCAGGS vector containing the HIV-1 or HIV-2 *gag* gene with a Flag epitope sequence, and after incubation at 37°C for 48 h, cells and culture medium were harvested for analysis. The culture medium was subjected to centrifugation on 20% sucrose cushions for purification of Gag VLPs. (A) Intracellular Gag expression and Gag VLP production. Transfected cells and Gag VLP fractions were subjected to SDS-PAGE followed by Western blotting using anti-Flag antibody. Lanes: M, molecular weight markers; 1 and 2, expression of HIV-1 and HIV-2 Gag-Flag, respectively. (B) Membrane affinity of Gag. Transfected cells were resuspended in buffer without NaCl and disrupted by sonication. Equilibrium flotation centrifugation and subsequent fractionation were carried out as described in the legend for Fig. 4. The gradient fractions were analyzed by Western blotting using anti-Flag antibody. Panels: 1, cells expressing HIV-1 Gag-Flag; 2, cells expressing HIV-2 Gag-Flag. (C) Sedimentation analysis of Gag. The whole-cell lysate was subjected to sedimentation analysis with a 20 to 70% sucrose gradient by centrifugation at 120,000 × *g* for 2 h, and gradient fractions were subjected to Western blotting using anti-Flag antibody. Panels: 1, cells expressing HIV-1 Gag-Flag; 2, cells expressing HIV-2 Gag-Flag. Arrowheads show sedimented positions of the immature form of HIV capsid (600S) and of 80S ribosomes.

membrane and formed high-order Gag multimers in higher eukaryotic cells and thus that no defect of particle production was observed.

The helix 2 region, but not the trimerization site, in HIV-2 MA abolishes high-order Gag assembly and subsequent particle production in yeast. To map a Gag region responsible for the failure of particle production in yeast, a series of chimeric Gag constructs between HIV-1 and HIV-2 were made (Fig. 7A) and expressed in yeast. Western blotting using anti-HIV-1 and anti-HIV-2 CA antibodies confirmed that each domain of Gag was replaced in the chimeric constructs. Spheroplast formation and VLP production were carried out as described above. Equivalent volumes of Gag VLP fractions were analyzed by SDS-PAGE followed by CBB staining. A failure of particle production was observed only when HIV-2 MA was present in the constructs (Fig. 7B, left panels). Further mapping experiments within MA indicated that the N-terminal one-third of HIV-2 MA (amino acid residues 1 to 44) is essentially responsible for the failure of VLP production (Fig. 7B, right panels). However, introduction of the corresponding region of HIV-1 MA into the HIV-2 background [construct M1(1/3)] did not rescue particle production, but a larger region of HIV-1 MA (the N-terminal half; residues 1 to 70) was required for particle production. Conversely, introduction of the N-terminal half of HIV-2 MA into the HIV-1 background [construct M2(1/2)] did not completely abolish particle production, but the introduction of a larger region of HIV-2 MA [construct M2(2/3)] did. These data suggest but do not prove that other sites affecting particle production may lie in the region between residues 45 and 96 and that the overall structural integrity of MA is not negligible.

Studies by nuclear magnetic resonance (25, 26) and crystallography (18, 38) have indicated that primate lentiviral MAs share three-dimensional characteristics, including the following: (i) the globular domain is composed of five helices (H1 to H5) capped by a β-sheet, in which the N-terminal basic residues are clustered; and (ii) in the MA trimer, the N-myristoyl moiety is inserted into a lipid bilayer and the surface-exposed basic residues come into contact with acidic phospholipids, such as phosphatidylinositol 4,5-bisphoshate [$PI(4,5)P_2$], in the membrane (18, 41). Indeed, the gross conformation of HIV-2 MA predicted by homology modeling using the SIVmac MA structure (38) as a template at Geno3D, an automated protein-modeling Web server (http://geno3d-pbil.ibcp.fr), is very similar to that of HIV-1 MA (see the supplemental material at http://www.kitasato-u.ac.jp/lisci/labo/ViralInfection2/1/Fig.S1.pdf), and the N-terminal half of MA (e.g., the cluster of basic amino acids) is relatively conserved between HIV-1 and HIV-2 compared with the C-terminal half (see the supplemental material at the website listed above), but our study found that the N-terminal half of MA is a determinant for Gag VLP production in yeast. To define the residues of MA critical for particle production in yeast, the clusters of nonconserved HIV-1 residues in the N-terminal half of MA were replaced with the corresponding HIV-2 residues (Fig. 8A), and the Gag constructs were expressed in yeast. Most of the substitutions had little effect on VLP production, and nearly equivalent levels of VLPs were produced even in the substitution mutant of the N-terminal trimerization site [construct 1(GLA)]. Interestingly, VLP production was severely impaired by the introduction of HIV-2 residues 38 to 40,